

Award Number: **W81XWH-11-1-0241**

TITLE: **Determining Changes in Neural Circuits in Tuberous Sclerosis**

PRINCIPAL INVESTIGATOR: **Mark Zervas, Ph.D.**

CONTRACTING ORGANIZATION: **Brown University**
Providence, RI 02912

REPORT DATE: **May 2012**

TYPE OF REPORT: Annual

PREPARED FOR: **U.S. Army Medical Research and Materiel Command**
Fort Detrick, Maryland 21702-5012

DISTRIBUTION STATEMENT: **Approved for Public Release;**
Distribution Unlimited

The views, opinions and/or findings contained in this report are those of the author(s) and should not be construed as an official Department of the Army position, policy or decision unless so designated by other documentation.

REPORT DOCUMENTATION PAGE			<i>Form Approved</i> OMB No. 0704-0188		
Public reporting burden for this collection of information is estimated to average 1 hour per response, including the time for reviewing instructions, searching existing data sources, gathering and maintaining the data needed, and completing and reviewing this collection of information. Send comments regarding this burden estimate or any other aspect of this collection of information, including suggestions for reducing this burden to Department of Defense, Washington Headquarters Services, Directorate for Information Operations and Reports (0704-0188), 1215 Jefferson Davis Highway, Suite 1204, Arlington, VA 22202-4302. Respondents should be aware that notwithstanding any other provision of law, no person shall be subject to any penalty for failing to comply with a collection of information if it does not display a currently valid OMB control number. PLEASE DO NOT RETURN YOUR FORM TO THE ABOVE ADDRESS.					
1. REPORT DATE 01-05-2012		2. REPORT TYPE Annual		3. DATES COVERED 15 April 2011 - 14 Apr 2012	
4. TITLE AND SUBTITLE Determining Changes in Neural Circuits in Tuberous Sclerosis			5a. CONTRACT NUMBER		
			5b. GRANT NUMBER W81XWH-11-1-0241		
			5c. PROGRAM ELEMENT NUMBER		
6. AUTHOR(S) Mark Zervas E-Mail: mark_zervas@brown.edu			5d. PROJECT NUMBER		
			5e. TASK NUMBER		
			5f. WORK UNIT NUMBER		
7. PERFORMING ORGANIZATION NAME(S) AND ADDRESS(ES) Brown University Providence RI 02912-9079			8. PERFORMING ORGANIZATION REPORT NUMBER		
9. SPONSORING / MONITORING AGENCY NAME(S) AND ADDRESS(ES) U.S. Army Medical Research and Materiel Command Fort Detrick, Maryland 21702-5012			10. SPONSOR/MONITOR'S ACRONYM(S)		
			11. SPONSOR/MONITOR'S REPORT NUMBER(S)		
12. DISTRIBUTION / AVAILABILITY STATEMENT Approved for Public Release; Distribution Unlimited					
13. SUPPLEMENTARY NOTES					
14. ABSTRACT The purpose of our research proposal is to unravel how neural circuits and neuronal physiology of the thalamus contribute to brain dysfunction in Tuberous Sclerosis. The major findings during the research period are that we temporally controlled <i>Tsc1</i> gene deletion at two distinct time points in thalamus development. Our strategy results in a mosaic distribution of mutant neurons in adult mice. Using genetic circuit mapping along with temporal gene deletion, we show that <u>early <i>Tsc1</i> deletion</u> results in ectopic parvalbumin-expressing thalamic axons that exit the thalamus and coalesce in the striatum. In addition, mutant thalamic axons reach, but do not properly innervate, the cerebral cortex. These alterations underlie aberrant repetitive grooming abnormalities and seizures that were present in all eleven conditional mutant mice. Importantly, the early deletion of <i>Tsc1</i> in the thalamus mimicked salient features of human Tuberous Sclerosis including mosaicism, autism and epilepsy. In contrast, <u>later <i>Tsc1</i> deletion</u> did not cause repetitive grooming abnormalities and seizures in only two of seventeen mice. We have determined base line physiological properties from thalamic neurons in which one copy of <i>Tsc1</i> is deleted. <i>Therefore, a novel and significant finding is that we identified a short temporal developmental window where <i>Tsc1</i> deletion in the embryonic thalamus causes deficits in thalamocortical neural circuit architecture concomitant with behavioral abnormalities.</i>					
15. SUBJECT TERMS Temporal gene deletion and genetic circuit mapping, Genetic neuroanatomy, Mouse model of Tuberous Sclerosis, Spatially and temporally controlled mosaicism					
16. SECURITY CLASSIFICATION OF:			17. LIMITATION OF ABSTRACT	18. NUMBER OF PAGES	19a. NAME OF RESPONSIBLE PERSON
a. REPORT	b. ABSTRACT	c. THIS PAGE			USAMRMC
U	U	U	UU	56	19b. TELEPHONE NUMBER (include area code)

Table of Contents

	<u>Page</u>
Introduction.....	1
Body.....	1
Key Research Accomplishments.....	10
Reportable Outcomes.....	10
Conclusion.....	11
References.....	13
Appendices.....	Appendix 1, P. 18 (24 pages)
	Appendix 2, P. 42 (15 pages)

INTRODUCTION

The purpose of our research proposal is to unravel how neural circuits and neuronal physiology of the thalamus contribute to brain dysfunction in Tuberous Sclerosis. The major findings during the research period are that we showed the ability to temporally control *Tsc1* gene deletion at two distinct time points in thalamus development. Our strategy results in a mosaic distribution of mutant neurons in adult mice. Using genetic circuit mapping along with temporal gene deletion, we show that early *Tsc1* deletion results in ectopic parvalbumin-expressing thalamic axons that exit the thalamus and coalesce in the striatum. In addition, mutant thalamic axons reach, but do not properly innervate, the cerebral cortex. These alterations underlie aberrant repetitive grooming abnormalities and seizures that were present in all eleven conditional mutant mice. Importantly, the early deletion of *Tsc1* in the thalamus mimicks salient features of human Tuberous Sclerosis including tissue mosaicism, autism, and epilepsy. In contrast, later *Tsc1* deletion does not cause repetitive grooming abnormalities in any mice and seizures in only two of seventeen mice. We also determined base line physiological properties from thalamic neurons in which one copy of *Tsc1* is deleted. *Therefore, a novel and significant finding is that we identify for the first time a short temporal developmental window where *Tsc1* deletion in the embryonic thalamus causes deficits in thalamocortical neural circuit architecture concomitant with behavioral abnormalities.*

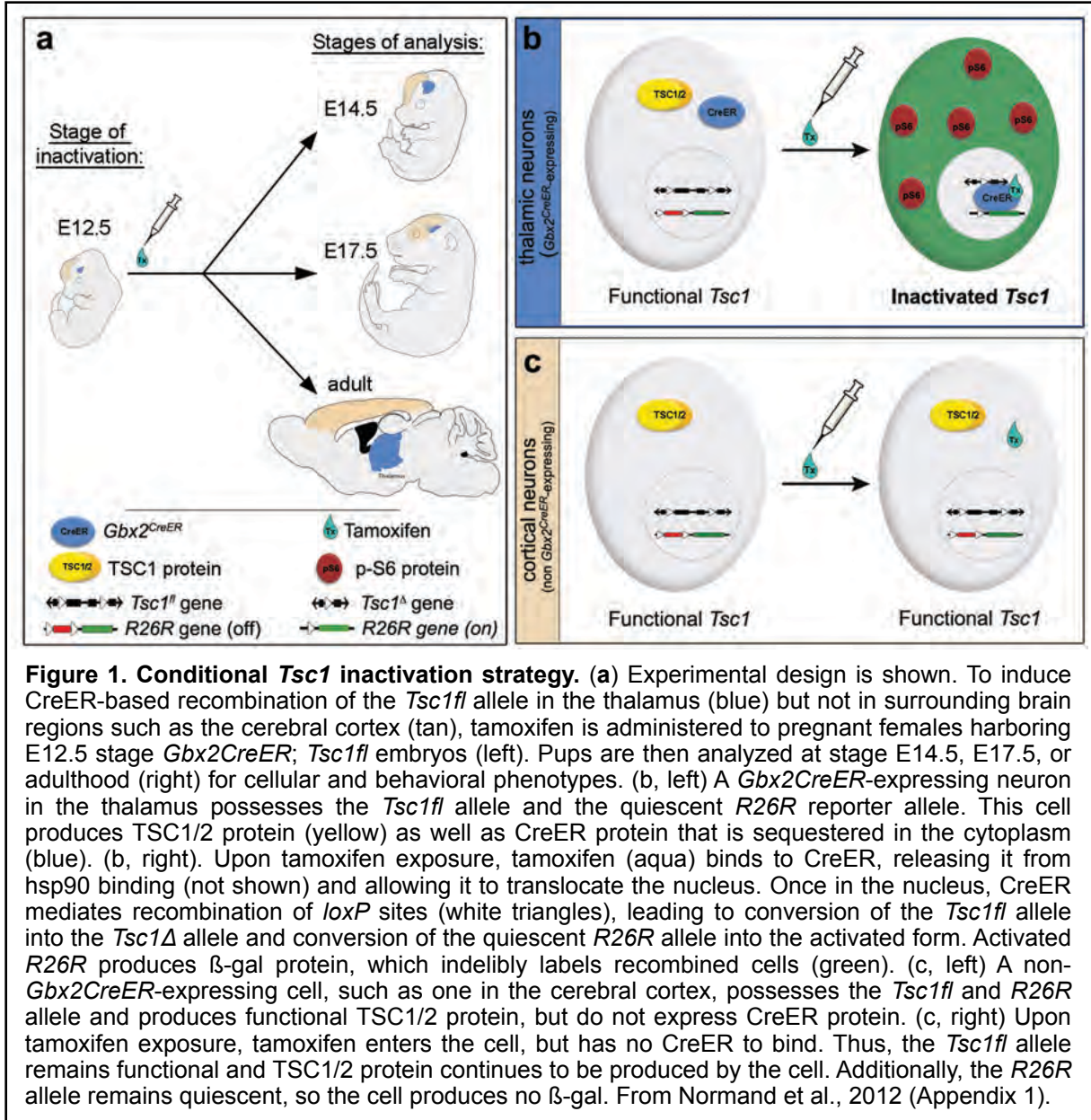
BODY

The information extracted from our proposed research “Determining Changes in Neural Circuits in Tuberous Sclerosis” has advanced our understanding of brain dysfunction in human Tuberous Sclerosis (TS). TS is a genetic mosaic disorder in which the inheritance of a mutant allele of one copy of the *Tsc1* gene is subsequently paired with a second somatic mutation that renders cohorts of cells with the complete loss of function of *Tsc1*. Notably, this situation results in a mosaic tapestry of mutant and otherwise unaffected cells. The loss of function of *Tsc1* in the brain may cause mental retardation, seizures, sleep disorders, and autism. We focused on testing how a mosaic distribution of mutant neurons in the thalamus affects thalamocortical circuits and function. We chose the thalamus because it integrates sensory information and modulates the cerebral cortex and is absolutely critical for proper brain function. Notably, the thalamus is an epicenter that synchronizes information processing and generates rhythmic activity. Not surprisingly, the thalamus is a focal point of research related to aberrant electrical activity in the brain underpinning epilepsy and seizures, both of which are prominent in TS. More directly, in recent study, patients with TS have been shown to have structural changes in the thalamus that is tightly linked to poor performance on cognitive tasks (Ridler et al., 2001). In addition, the thalamus has been linked to the autism component in human TS (Asano et al., 2001). The information presented above indicates that the thalamus is poised to play an important role in brain dysfunction in TS. The importance of the thalamus is reflected by an excerpt from a recent book: Tuberous Sclerosis Complex Genes, Clinical Features, and Therapeutics edited by D. Kwiatkowski, V. Whittemore, and E. Thiele (2010).

“a comprehensive analysis of structural alterations in subcortical regions such as the thalamus [...] will likely identify potential cytoarchitectural substrates that contribute to cognitive disabilities in TSC.”

We have taken advantage of sophisticated genetic approaches in mice (Joyner and Zervas 2006, Brown et2009; Ellisor 2009) that we described in the initial application and have now advanced the foundation technology in a novel system that allows for the deletion of *Tsc1* with fine temporal and spatial control while also genetically marking mutant neurons and their

axons. Thus, we are in a position to link genetic mutations directly to neural circuits. It is important to note that the mutant thalamic circuits that we analyze are in the context of *Tsc1* loss in the thalamus while surrounding brain regions are genetically and phenotypically normal (Figure 1 and Normand et al., 2012 (See Appendix 1 for genetic approach and experimental details)).



The first task we proposed in our Statement of work was to ascertain the developmental profile of thalamocortical circuitry in *Tsc1* conditional mutant mice. Specifically, we proposed to assess axonal projections of *Tsc1*-deficient neurons located in the thalamus as they innervate their target sites in cortex. We made significant progress on this aim with two approaches: First we deleted *Tsc1* and quantified thalamic axons that had been labeled by lentivirus engineered to express a fluorescent reporter thalamic nuclei. Second, we used a genetic reporter allele to

monitor mutant thalamic neurons. In both approaches, the *Gbx2* lineage in the thalamus was marked concomitant with conditional gene deletion of *Tsc1* using *Gbx2^{CreER};R26R;TSC1^{f/f}* mice as shown in Figure 1. With the first approach, subsequent to deleting *Tsc1* in the developing thalamus, we locally infected the ventral-posterior-medial nucleus in the thalamus with lentivirus-YFP (yellow fluorescent protein, which is detected with a GFP antibody) and quantified the thalamocortical innervation (Figure 2). We chose this nucleus of the thalamus because of its well-defined projections to somatosensory cortex (Meyer et al., 2010). We previously showed that this approach allowed us to label control versus mutant thalamocortical circuits of anatomically distinct thalamic nuclei (Figure 2A,F). The delivery of lentivirus resulted in fluorescently-labeled neurons localized to the injection site; the reporter was then anterogradely transported along thalamocortical axons, which could be seen as a rich plexus and an overlying lattice of well-organized fascicles that innervated the cerebral cortex in controls (Figure 2B-D). In contrast, thalamic projections in mutants had a less extensive axonal plexus and de-fasciculated bundles that innervated the cortex in a disorganized pattern (Figure 2F-I). We now quantified the Innervation of the layer 4 barrels in somatosensory cortex, which was readily identified in control and conditional *Tsc1* heterozygotes (Figure 2E, data not shown). In contrast, the conditional deletion of both copies of *Tsc1* resulted in thalamocortical axons that were enriched in layer 5b, but not in layer 4 (Figure 2J). The 25% reduction in the innervation of layer 5 and complementary increase in the deeper layer 5b resulted in a “softening” of the somatosensory barrels (Figure 2E and J).

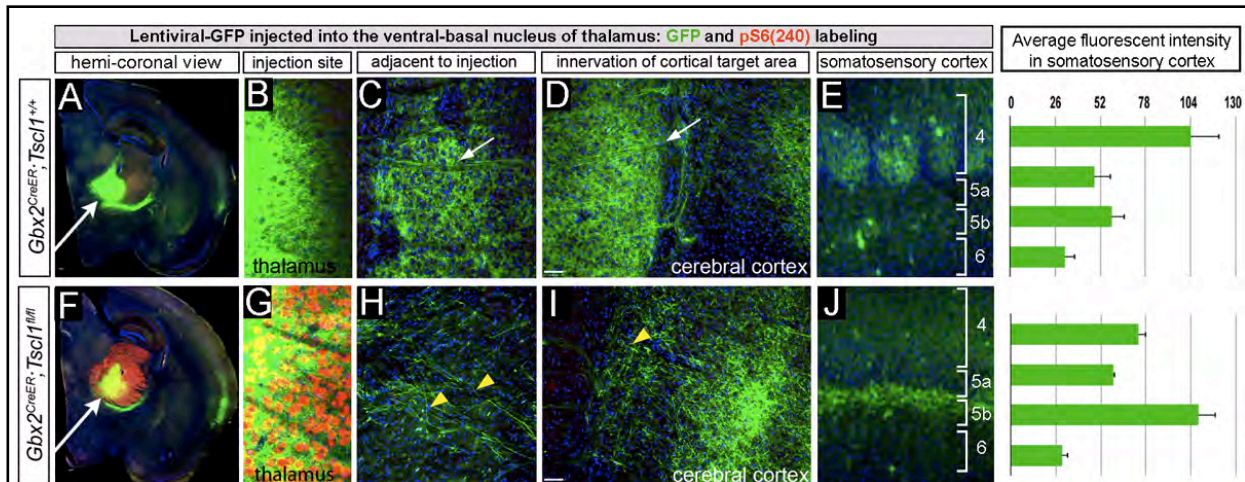
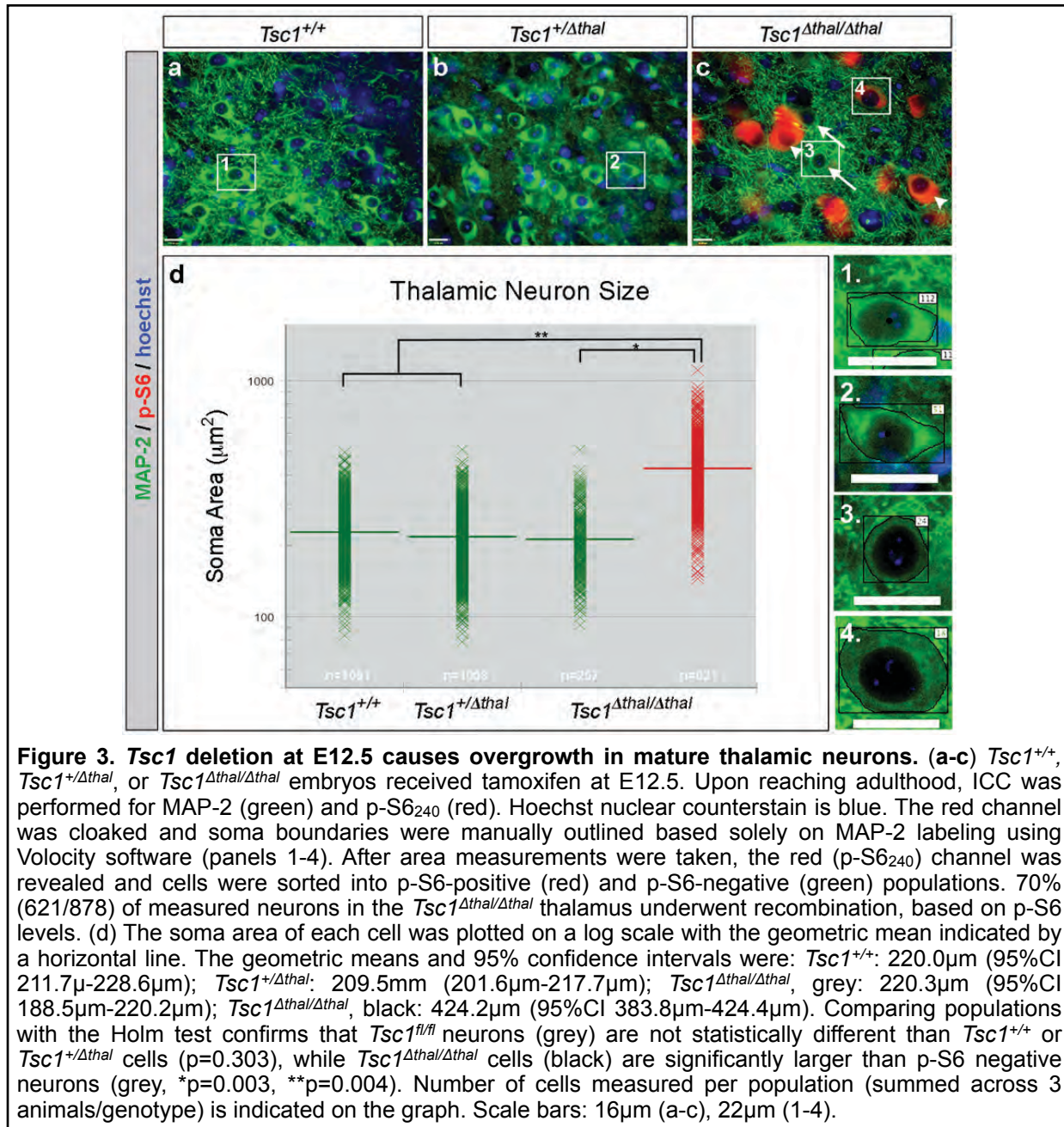


Figure 2. *Tsc1* deletion in the developing thalamus causes aberrant thalamocortical circuits.

Lentivirus-GFP (green; 0.5 μ l of virus, titer 10^{10} IU/ml) was delivered to the VPM nucleus of the thalamus [coordinates from Bregma: -1.94 (R-C), 1.56 (M-L), 3.50 (depth)] of control (A-E) and conditional *Tsc1* mutants (F-J) by stereotaxic surgery. The injection in VPM of thalamus in control (A,B) and mutants (F,G) was distinguished by GFP labeling. The conditional deletion of *Tsc1* in the thalamus was evident by pS6₂₄₀ + (red). Controls had well organized axon bundles that could be traced to the target site (C,D). *Tsc1* mutants had disorganized and de-fasciculated projections (H,I) that randomly entered the cortex (I). The ventral-posterior-medial nucleus projects to the somatosensory cortex and innervates barrel structures in layer 4 of controls (E). *Tsc1* conditional mutants did not properly innervate somatosensory cortex barrels (J). Graphs show fluorescent intensity in the indicated layers: Note the 30% reduction in the barrel layer (4) and 46% increase in layer (5b), which appeared to have axons that failed to enter the more superficial layers. From Normand et al., 2012 (Appendix 1).

While this allelic combination and lentivirus approach has the advantage of being able to visualize the mutant thalamic neurons based on pS6₂₄₀ labeling and marking specific nuclei in

the thalamus, what it lacks is the ability to identify whether the disorganized axons are from mutant thalamic neurons or represent the combination of mutant and unaffected axons that were dragged along with mutant axons. This is an important consideration because our genetic approach results in a mosaic tapestry of 70% mutant (enlarged pS6₂₄₀⁺) and 30% unaffected (normal size, pS6₂₄₀⁻) neurons (See Figure 3 and Normand et al., 2012, Appendix 1). While mosaicism complicates the experiments shown in Figure 2, they are a distinct advantage experimentally because human TS is a genetic mosaic disorder; thus we are recapitulating a salient cellular feature of TS in our novel mouse model.



To overcome the limitation of linking the *Tsc1* gene deletion with mutant axons, we substituted the *R26*^{tdTomato} reporter for the *R26R*^{LacZ} allele because *R26*^{tdTomato} encodes a red

fluorescent protein that fills axons (Madison et al., 2010, Hagan et al., 2012, Normand et al., 2012, Normand et al., 2012a, Appendices 1 and 2). We initially deleted *Tsc1* at E12.5 and analyzed the adult thalamocortical circuits marked genetically to compare directly with our lentiviral labeling approach (compare Figure 3 and Figure 4). In control animals, thalamocortical axons innervated layer 4 whisker barrels in somatosensory cortex, with synapses located in discrete clusters corresponding to individual whiskers, similar to descriptions from studies using non-genetic labeling methods. In contrast, *Tsc1^{Δthal/Δthal}* mice had a noticeably more diffuse pattern of whisker barrel cortical innervation (Figure 4a,b). Within the internal capsule of the *Tsc1^{Δthal/Δthal}* brains, thalamocortical axon fascicles also appeared more diffuse and disorganized compared to controls (Figure 4a,b). In addition to this disorganization, we detected aberrant parvalbumin (PV) expression in fibers within the internal capsule of *Tsc1^{Δthal/Δthal}* brains, which was not apparent in *Tsc1^{+/+}* or *Tsc1^{+/Δthal}* controls (Figure 4c-g). The reason this is important is that PV+ neurons are a class of thalamic relay neurons and we thus showed that a type of neuron is sensitive to *Tsc1* deletion. The spatial location of these fibers, the lack of recombination within the nearby PV+ thalamic reticular nucleus, and the presence of PV+/β-gal + cell bodies in the thalamic relay nuclei (Figure 4e,h) strongly suggested that these fibers were

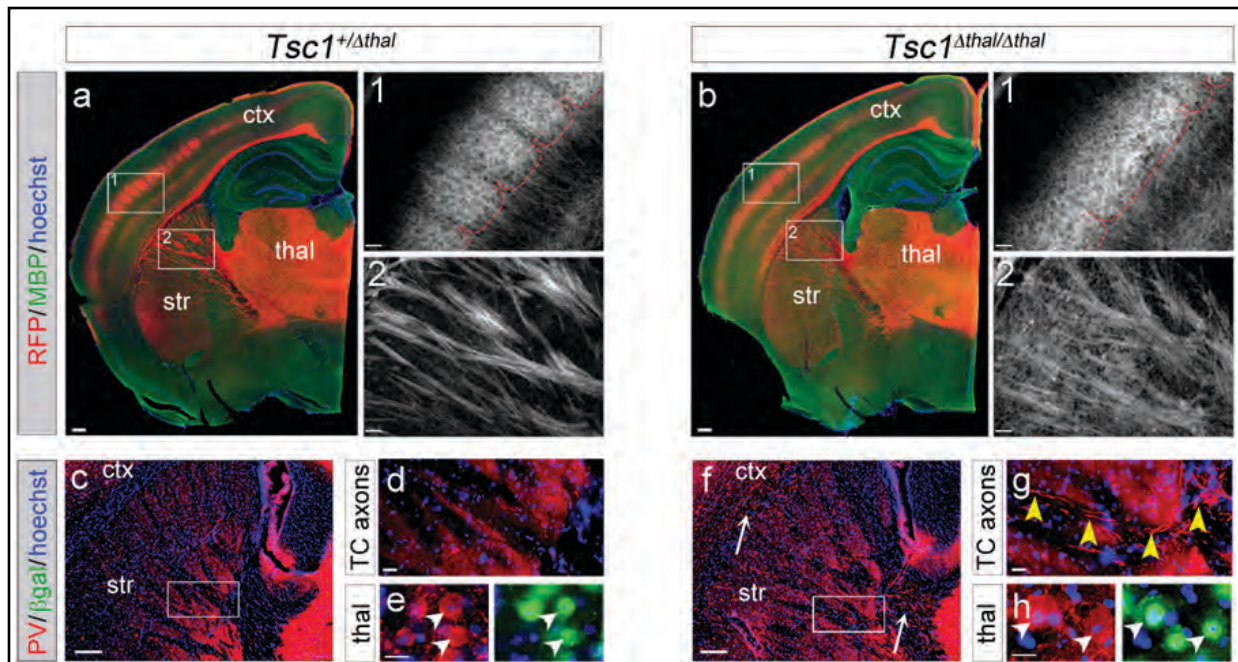
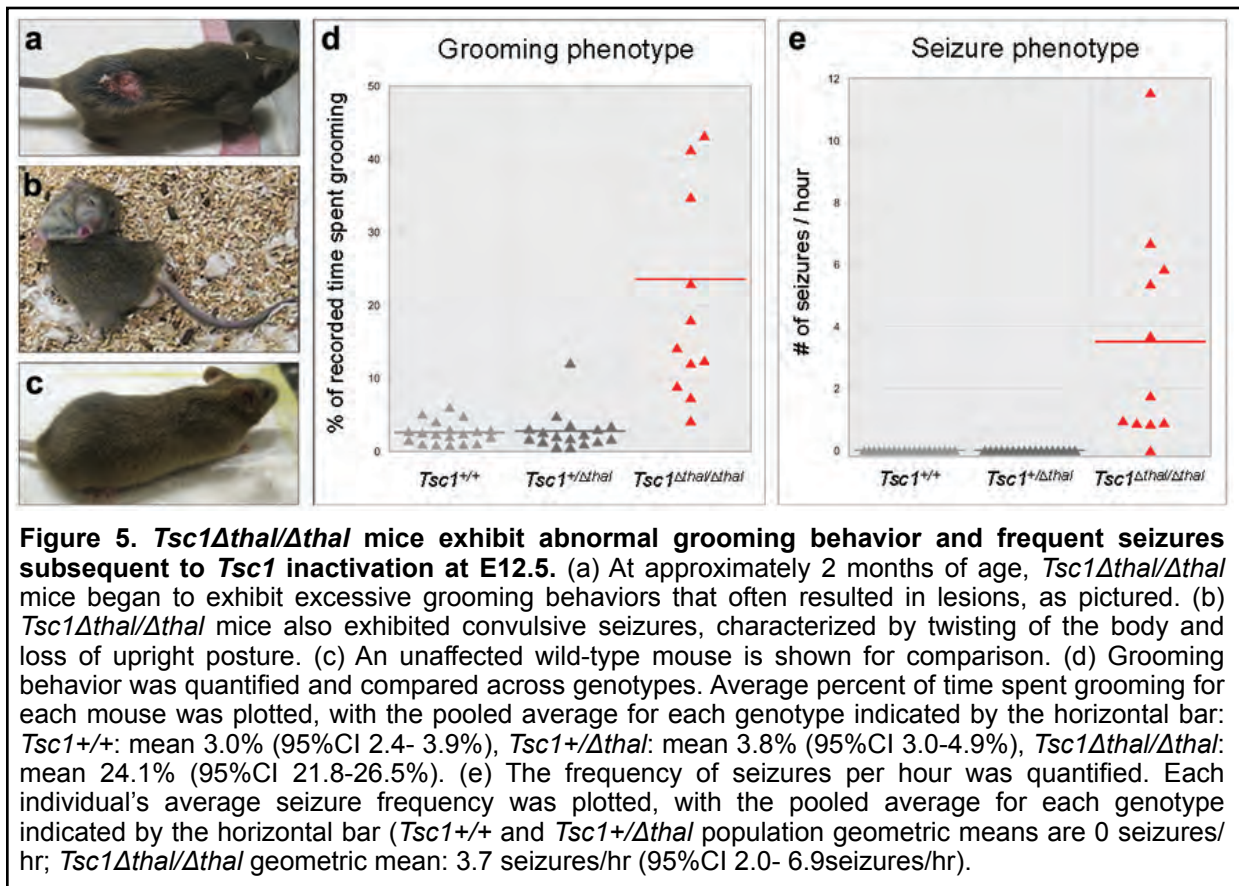


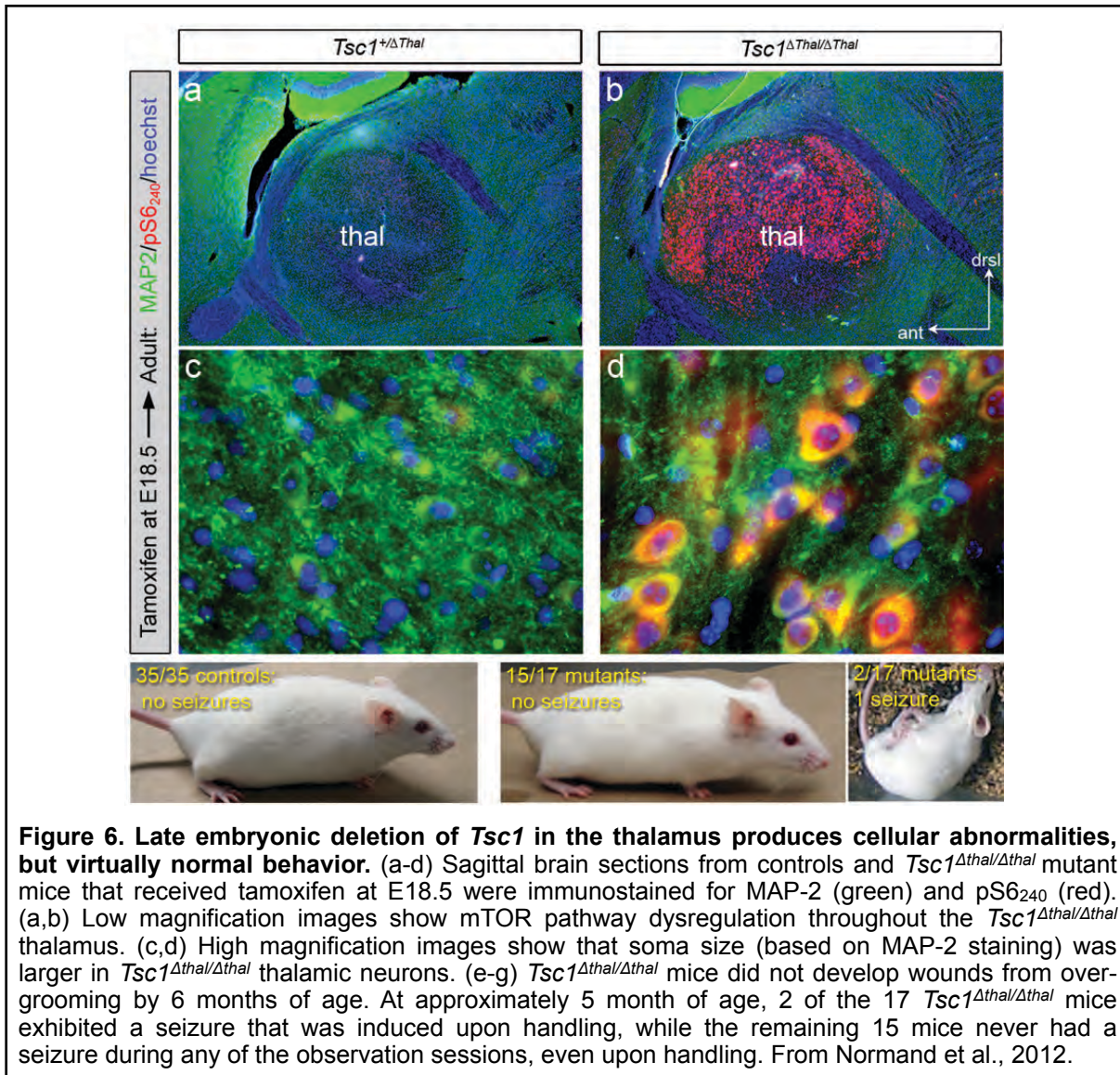
Figure 4. *Tsc1^{Δthal/Δthal}* mutants have abnormal thalamic circuits. Tamoxifen was administered at E12.5 to induce recombination of the *Tsc1^{fl}* allele. (a-b) ICC was performed to detect MBP (green) and the *tdTomato* reporter protein, RFP (red). MBP levels did not differ between controls and mutants. RFP+ thalamocortical innervation of whisker barrels was highly organized and discrete in control animals (a1), but is more diffuse in *Tsc1^{Δthal/Δthal}* mutants, where individual barrels were less apparent (b1). Within the internal capsule of *Tsc1^{Δthal/Δthal}* brains, thalamic axons bundles were also less sharply defined (b2). (c-h) ICC was performed for parvalbumin (PV, red) and β-gal (green). Hoechst 33342 nuclear counterstain, blue. (c,f) PV staining can be seen lateral to the thalamus, within the internal capsule, and in the external capsule (white arrows) of *Tsc1^{Δthal/Δthal}* brains (f), but was absent in *Tsc1^{+/Δthal}* or *Tsc1^{+/+}* control brains (c, data not shown). (d,g) High magnification images from the boxed regions in c,f showed that axon bundles within the internal capsule of the mutant brain contained PV+ fibers (yellow arrowheads) that were not seen in controls (d). Thalamic relay cell bodies were double positive for PV and β-gal (white arrowheads), raising the possibility that the PV fibers originate from PV-expressing *Tsc1^{Δthal/Δthal}* relay cells. Scale bars: 240mm (a,b); 61μm (a1,2 and b1,2); 180μm (c,f); 30μm (d,g); 15μm (e,h). thal, thalamus; str, striatum; ctx, cerebral cortex. From Normand et al., 2012.

thalamic axons from relay neurons. However, locally projecting neurons in the thalamic reticular nucleus (TRN) also express PV; notably the TRN is not marked with the *Gbx2^{CreER}* line. Therefore, to definitively identify the source of the aberrant projections, we immunolabeled sections with antibodies that showed that tdTomato+ axons were also PV+ and were therefore from the relay neurons and not TRN neurons passively swept into the internal capsule. Thus, in the absence of *Tsc1* the relay neurons have thick PV+ axons that exit the thalamus and enter the internal capsule. Because previous TS mouse models have described decreased cortical myelination we assayed for myelination (MBP) in the *Tsc1^{Δthal/Δthal}* thalamus. Control mice had clear MBP labeling throughout the brain, including within the thalamus and the internal capsule (Figure 4a). MBP labeling was not different in *Tsc1^{Δthal/Δthal}* mutant brains (Figure. 3b). Thus, aberrant PV+ thalamocortical axons exit the thalamus, yet thalamocortical axons do appropriately innervate somatosensory cortex properly and are not compromised by myelination defects.



We are now combining our genetic circuit mapping and lentiviral delivery to combine the ability to identify thalamic axons that are associated with the *Tsc1* deletion in thalamic neurons and the ability to identify which nuclei within the thalamus are most affected. Using multiple approaches, we showed that the loss of *Tsc1* in the thalamus has a direct consequence on how functionally related brain regions are connected. An important and clinically relevant question is what does this mean for the mice? At the time that we submitted the proposal, we speculated that this circuit abnormality might result in altered behavior. We showed that the loss of *Tsc1* in the thalamus results in repetitive motor behavior abnormalities and robust, frequent seizures (See Figure 5 and Normand et al., 2012, Appendix 1).

As part of Aim 1 and in our Statement of Work, we proposed to examine how neural circuits changed as a function of developmental time. To address this goal, we used our genetics based approach to delete *Tsc1* at an additional time point, which was at the end of embryonic development. We choose this stage because thalamic axons have already left the thalamus (See Normand et al., 2012a for details, Appendix 2). Therefore we administered tamoxifen to pregnant females harboring embryos at the end of embryogenesis and analyzed them at adulthood. Similar to the early deletion, we could readily detect enlarged pS6+ neurons in the thalamus of conditional mutants while control littermates showed normal size and very low levels of pS6₂₄₀ (Figure 6a-d). This is an important control to show that thalamic neurons do indeed undergo recombination with late administration of tamoxifen and that the mTOR pathway is dysregulated as a result of deleting *Tsc1* in the thalamus. In contrast to the early deletion in which neural circuits and behavior were altered, the late deletion did not result in grooming abnormalities and only two out of seventeen mice had seizures (Figure 6). We are now applying our circuit mapping approaches to determine whether subtle changes in neural circuitry accompany the two mice that had seizures.

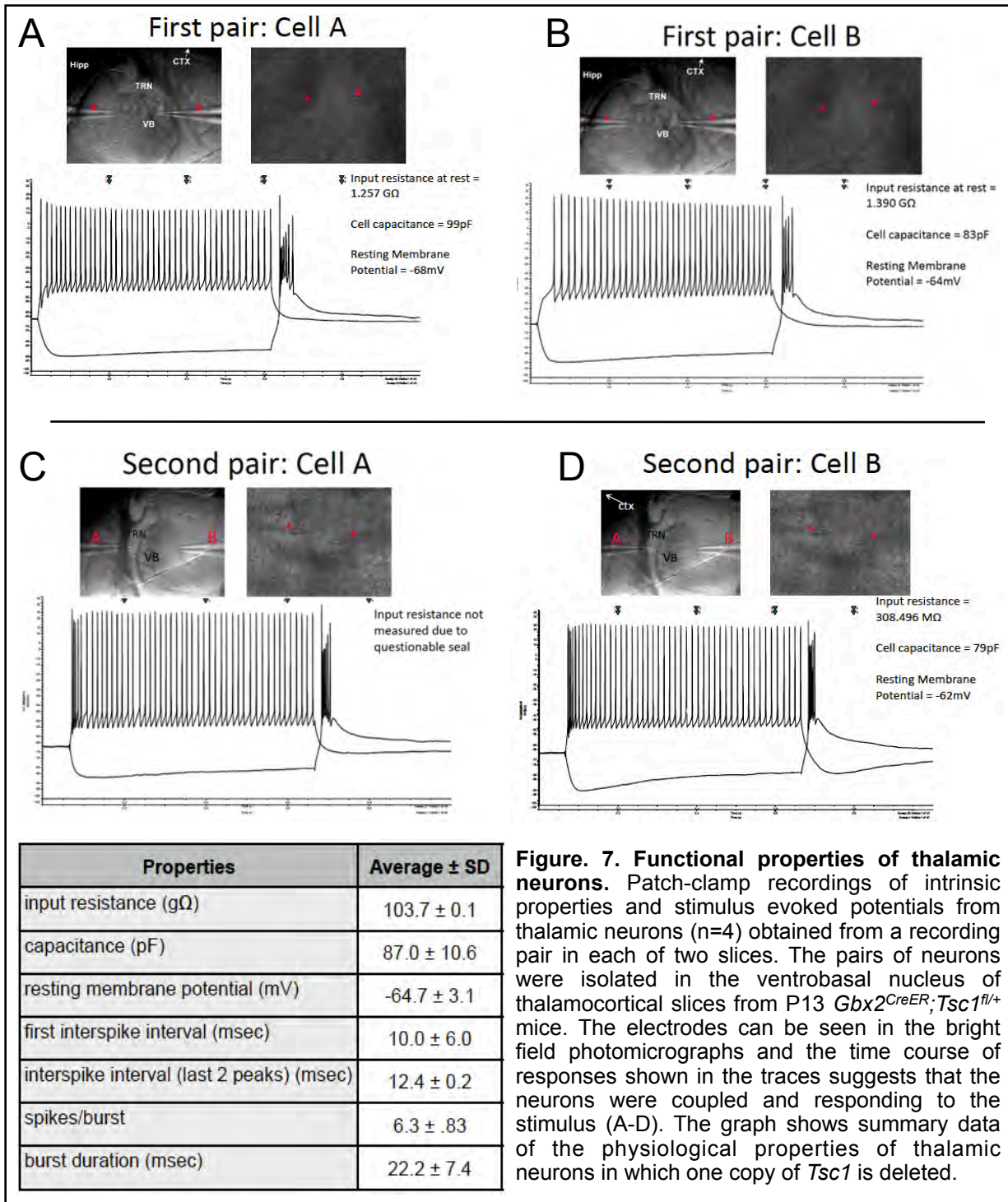


In this report we now compare for the first time, the mosaic deletion of *Tsc1* at two distinct time points (early and late embryonic development) in the same structure (thalamus). Therefore, one of the product/deliverables that described in our initial Statement of Work that has been provided through this first grant period is a complex allelic line of mice (*Gbx2^{CreER/+};R26^{tdTomato/+};Tsc1^{fl/fl}*) that is available to the TS and Neuroscience community and can be used to evaluate pharmacological approaches to diminish the affects of *Tsc1* loss of function and rescue of the proper establishment of this neural circuit. We have two manuscripts related to this project. The first describes the use of conditional gene deletion and marking and tracking neural circuits (Normand et al., 2012a, Appendix 2) and the second is a direct application of conditional gene deletion and circuit mapping to show a sensitive time period whereby *Tsc1* deletion causes neural circuit changes and behavioral abnormalities (Normand et al., 2012, Appendix 1). We recently an award to use these mice and the concept of circuit mapping to ascertain how mTOR inhibitors cn rescue neural circuits disrupted by *Tsc1* deletion (See Reportable Outcomes, below).

The second task in our Statement of Work was to begin to determine whether the intrinsic circuitry physiology of the thalamus is altered in *Tsc1* conditional mutant mice and whether this impacts the cerebral cortex (target site). A combination of GIFM, gene inactivation, and electrophysiology was proposed to delineate whether specific cohorts of *Tsc1*-deficient neurons in the thalamus affects the physiology of the developing neural circuits. We have initiated and conducted pilot experiments in which thalamocortical slices were obtained from postnatal day (P)13 *Gbx2^{CreER};Tsc1^{fl/+}* mice that had one copy of *Tsc1* deleted by tamoxifen administration at E12.5 (Figure 7).

The *Gbx2^{CreER};Tsc1^{fl/+}* slices, which were 300 μm thick and 35° tilt from coronal consistent with previous reports (Agmon and Connors 1991), were incubated in artificial cerebrospinal fluid in a submersion recording chamber at 32°C. Preliminary experiments demonstrate that we can readily prepare thalamocortical slices from postnatal day (P)7 *Gbx2^{CreER};Tsc1^{fl/+}* mice and record physiological properties from pairs of neurons (Figure 7A-D and Figure 7 Table). We performed whole cell patch clamp recordings and measured resting properties including input resistance, capacitance, and resting membrane potential (Figure 7A-D and Figure 7 Table). We will continue to use 10pA steps of current injection to hyperpolarize individual neurons. The same neurons will then be depolarized using the same current steps. We will also apply stimulating currents (3 to 400 μA , 200 μsec duration) and trains of 4 shocks at a frequency of 40 Hz to evoke synaptic responses (Landisman et al., 2007). We recorded interspike intervals (tonic firing mode), the number of spikes/burst, and burst duration (after-hyperpolarization) (Figure 7, Table). Finally, inhibitory post synaptic potentials (IPSP) will be recoded at membrane potentials of -55 to -70 mV and evoked inhibitory post synaptic currents (IPSC) will be determined by applying square pulses of 20- μs duration at a frequency of 0.05 Hz, 10–40V to obtain IPSC amplitudes 1.5 times the threshold response. Recordings will be performed with Axon Instruments equipment and analyzed with Multiclamp 700B, Digidata 1440A, pClamp 10). Statistical significance will be determined with *t* tests.

In our statement of Work, we proposed to initiate the analysis of thalamic neuron properties using a slice preparation and we have met that goal. In this second year, we will utilize this method to analyze thalamic neurons in which both copies of *Tsc1* have been deleted and we will also stimulate control versus mutant thalamic neurons and record responses from the genetically unaffected somatosensory cortex (layer 4). This experiment will likely be very informative because the early deletion of *Tsc1* caused abnormal innervation of cortical layer 4.



KEY RESEARCH ACCOMPLISHMENTS

- Developed quantitative analysis of thalamic innervation of cortical target layers
- VPM thalamic nucleus does not have distinct somatosensory representation
- VPM thalamic axons are abrogated in deep cortical layers
- Genetic circuit mapping links genetically mutant thalamic neurons and axon deficiencies
- Ectopic PV+ projections from thalamic relay neurons enter striatum
- Thalamocortical axons reach but do not properly innervate cortical targets
- Early *Tsc1* deletion linked to altered neural circuits, seizures, and repetitive grooming
- Late *Tsc1* deletion causes only seizures and in only 2 out of 17 mice
- Established electrophysiological baseline in *Tsc1* heterozygous thalamic neurons

REPORTABLE OUTCOMES

Manuscripts

Normand E, Browning C, Machan JT, **Zervas M** (2012) Seizures and compulsive grooming behaviors resulting from thalamus-specific *Tsc1* gene inactivation. *Nature Medicine*. Manuscript #NMED-A60580, Submitted.

Normand E, Browning C, Hagan N, **Zervas M** (2012) Genetic marking of neural circuits. *Gene Exp Patterns*, Submitted.

Abstracts

Normand E, **Zervas M** (2011) Developmental and behavioral results of a *Tsc1*-null thalamus in an otherwise normal brain. *International TSC Research Conference: Summit for Drug Discovery in TSC and Related Disorders*. July 6-9, 2011, Washington DC. Student Travel Award.

Rios M, Normand E, **Zervas M** (2011) The effects of rapamycin treatment on *Tsc1*-deficient neurons in the thalamus. *BP-ENDURE at Hunter/NYU Neuroscience Research Symposium*. July 29-31, 2011.

Normand E, **Zervas M** (2011) mTOR pathway dysregulation during thalamic development leads to severe behavioral abnormalities in adult mice. *Mammalian Development Meeting*. September 2, 2011, UCHC, CT. Student Presentation.

Normand E, Browning C, **Zervas M** (2012) Cellular and behavioral consequences of mTOR pathway dysregulation within a population of subcortical neurons during mouse embryogenesis. *Keystone Symposia: Synapses and Circuits: From Formation to Disease*, Apr 1-6 2012, Steamboat Springs, Colorado. (* student travel award recipient).

Invited Seminars

M. Zervas. "Determining how the temporal and spatial deletion of *Tsc1* and mTOR dysregulation during brain development causes neurological disease in Tuberous Sclerosis". Honorary Lecturer at 8th Annual Pharmacology Graduate Students' Symposium, Stony Brook University. June 6, 2011 (Invited by Graduate Students).

M. Zervas. "Genetic Approaches in Mouse to Interrogate Brain Development and Disease". University of Massachusetts, Amherst, February 22, 2012 (Invited by Dr. Kim Tremblay, Ph.D.).

Funding applied for based on work supported by this award

TS110083 (PI: **Zervas, M**)

DOD-CDMRP Idea Development Award

Dates: 2012-2015 (Funded, June 1, 2012 start date)

Temporal loss of *Tsc1*: Neural development and brain disease in Tuberous Sclerosis

Role: Principal Investigator; Total Award: (direct costs)

The major goals of this project are to identify how critical windows of brain development are affected by the loss of *Tsc1*, how normal brain development is impacted by mTOR inhibition, and how the timing and duration of rapamycin ameliorates cellular, neural circuit, and behavioral changes in a conditional mouse model of Tuberous Sclerosis.

R01 Accession # 3459040 (PI: Zervas M)

NIH R01

Dates: Dec 01, 2012-November 30, 2017

Subcortical brain structures and neurological disease in Tuberous Sclerosis

Role: Principal Investigator; Total Award:

The major goals of this project are to conditionally delete *Tsc1* in the striatum during embryonic development and ascertain how FMRP phosphorylation and SAPAP3 protein expression are affected to link a molecular pathway to repetitive behaviors in a mouse model of Tuberous Sclerosis.

To be reviewed June 7-8.

Training supported by this award

Elizabeth Normand, Graduate Student in the Brown Neuroscience Graduate Program has been supported in part by this grant and has conducted the experiments described in this report. Elizabeth is also the first author on two recently submitted manuscripts that are related to this award. Elizabeth has presented her findings at three meetings and has received travel awards because of the high quality data and impact of her work.

CONCLUSION

Our research proposal uses an innovative approach based on a number of criteria including testing novel ideas, developing new animal model systems, and modifying existing molecular approaches to specifically address hypotheses relevant to neural circuitry and brain dysfunction in TS. It is clear that TS is a multi-systemic disorder that affects cognitive processing in a substantial cohort of TS patients. However, a thorough understanding of the affected brain regions, neuronal cell types, and neural circuits has not been ascertained in TS. In addition, the developmental progression of TS has not been elucidated. Finally, the developmental mechanisms causing brain disease in TS have not been carefully linked to aberrant neurological function at the cellular, circuit, or behavioral level. We have established an animal model that mimics salient features of TS and is an innovative advance to address deficiencies in TS research. Genetic approaches in mice allow us to test hypotheses that are central to understanding TS and we are using a sophisticated genetic method that I helped pioneer (Zervas et al., 2004, Brown et al., 2009, Ellisor et al., 2009, Ellisor et al., 2010) to induce genetic mutations and mark mutant neuronal populations with spatial and temporal control *in vivo*. We have successfully applied this methodology to inactivate *Tsc1* and mark mutant neurons including their axonal projections to target sites in development. Thus, innovative conceptual issues we have addressed are: 1. How specific populations of neurons are affected by *Tsc1* loss of function; 2. The structural and functional alterations occurring in thalamic neurons affected in

TS. 3. When *Tsc1* loss of function has its greatest impact on neuronal morphology and neural circuitry. This project proposes a new paradigm in which select neural circuits affected in TS are a critical predictor of the phenotype observed in specific brain regions. The findings represent more than an incremental understanding of TS by delineating the brain regions most likely affected in TS and by establishing which functionally connected regions are affected at the cellular level. In addition, the combination of mouse lines we are using will be beneficial to screen for therapeutic compounds designed to treat specific types of neurons and distinct neural circuits in TS. There is relatively little risk in the specific aims of this project because we are using a genetic approach that we have proven can mutate and mark cells *in vivo* with both temporal and spatial control. Specifically, our preliminary findings show that we can inactivate both alleles in the thalamus which causes a substantial increase in pS6₂₄₀, a statistically significant increase in thalamic neuron size, and disorganized thalamic-to-cerebral cortex axonal connections. Finally, the cellular and circuit changes are accompanied by behavioral abnormalities including robust and frequent seizures. The highly innovative nature of our approach is exemplified by performing: 1. The first temporally and spatially controlled biallelic deletion of *Tsc1*, 2. The first developmental study of changes in the developing brain in TS. 3. The first link between one specific brain region and a prominent behavioral change relevant to human TS. There are no significant changes that are required to better address the problems that we are addressing. However, we are taking advantage of both genetic circuit tracing and stereotaxic delivery of reporters to mark thalamic nuclei to identify mutant thalamic axons in subsets of nuclei. This is not a departure from our initially proposed work, but rather an evolution of using multiple approaches that we advanced during this research period, consistent with our Statement of Work, to precisely address alterations in thalamic circuitry.

This project is clinically relevant to TS because the gene that we are deleting (*Tsc1*) encodes hamartin (TSC1 protein) that forms a heterodimeric complex with tuberin (TSC2 protein). Together these proteins regulate downstream mammalian target of rapamycin (mTOR). The “mTOR pathway” is a central hub of intracellular signaling that is vital for cellular processes including cell growth, axon guidance, and transcriptional regulation (Crino 2004, Ess et al., 2006, de Vries et al., 2007, Swiech et al., 2008). Signal transduction through mTOR culminates in the phosphorylation of the ribosomal protein S6 (pS6), which is elevated to high levels when mTOR signaling is dysregulated. The genetic mechanism underlying TS is that patients inherit a loss of function allele of *Tsc1*. A subsequent second somatic mutation renders a clonally related population of cells devoid of functional *Tsc1* (Crino et al., 2010) and leads to mTOR dysregulation and an increase in pS6₂₄₀. We have begun to elucidate the role of *Tsc1*/mTOR in specific populations of neurons and identified a developmental timepoint and region particularly sensitive to *Tsc1* loss of function. Pharmacologically, the mTOR pathway can be suppressed by the drug rapamycin. However, a significant, clinically relevant problem to treating TS patients with rapamycin is the manner in which specific brain regions and cell types respond to *Tsc1* deletion and mTOR dysregulation and how mTOR inhibition may ameliorate these changes. Finally, the most effective time points to administer rapamycin have not been tested. Given the importance of mTOR in regulating developmental processes (Hentges et al., 2010), it is essential to control the timing of *Tsc1* deletion/mTOR dysregulation and to determine how rapidly and robustly neurons respond to rapamycin before considering this approach as a therapeutic paradigm for TS.

This project has made original and important contributions to advancing TS related research. First, we mutated neurons in selective brain regions with temporal control to isolate critical time periods that *Tsc1* inactivation is most pathogenic *in vivo*. Second, we simultaneously

marked mutant cells and traced axonal projections to identify changes in developing neural circuits related the loss of *Tsc1*. Third, we identified mutant neurons affected by *Tsc1* loss of function and subsequently determine the physiological changes occurring in mutant thalamic neurons. This project will positively affect TS research and possibly patient care by developing an animal model with both temporal and spatial control of *Tsc1* deletion that can we will use to test therapeutic approaches in a cell-type specific manner. This approach will be a foundation to test whether rapamycin is a viable treatment strategy to ameliorates specific features of TS and may be helpful to identify and test novel therapeutic targets for TS. My background in using animal models of neurological developmental brain disorders and therapeutic intervention in Niemann-Pick Disease Type C (NPC) led directly to human clinical trials to NPC. Thus, we have a track record of successfully conducting innovative approaches to understand brain diseases and show that our potential gains to uncover novel aspects of the developmental mechanisms underpinning TS greatly outweighs the perceived risk of using a complex genetic strategy. We have begun to establish a correlation between gene inactivation, changes in neural circuit structure, and physiology. Our animal model system will allow us to test the feasibility of pharmacological treatment strategies in ameliorating features of TS with an emphasis on how specific brain regions (thalamus) respond to rapamycin administration. We were recently awarded a grant to conduct the drug treatment studies.

REFERENCES

- Agmon, A., and Connors, B.W. (1991). Thalamocortical responses of mouse somatosensory (barrel) cortex in vitro. *Neuroscience* *41*, 365-379.
- Asano, E., Chugani, D.C., Muzik, O., Behen, M., Janisse, J., Rothermel, R., Mangner, T.J., Chakraborty, P.K., and Chugani, H.T. (2001). Autism in tuberous sclerosis complex is related to both cortical and subcortical dysfunction. *Neurology* *57*, 1269-1277.
- Brown A, Brown B, Ellisor D, Hagan, N, Normand, E, **Zervas, M.** (2009) A Practical Approach to Genetic Inducible Fate Mapping: A Visual Guide to Mark and Track Cells *In Vivo*. *J Vis Exp*, **43**: pii: 1687, doi: 10.3791/1687 (PMCID: PMC2846818).
- Crino, P.B. (2004). Molecular pathogenesis of tuber formation in tuberous sclerosis complex. *J Child Neurol* *19*, 716-725.
- Crino, P.B., Aronica, E., Baltuch, G., and Nathanson, K.L. (2010). Biallelic TSC gene inactivation in tuberous sclerosis complex. *Neurology* *74*, 1716-1723.
- de Vries, P.J., and Howe, C.J. (2007). The tuberous sclerosis complex proteins--a GRIPP on cognition and neurodevelopment. *Trends Mol Med* *13*, 319-326.
- Ellisor, D., Koveal, D., Hagan, N., Brown, A., and **Zervas, M.** (2009). Comparative analysis of conditional reporter alleles in the developing embryo and embryonic nervous system. *Gene Expr Patterns* *9*, 475-489.
- Ellisor D, **Zervas, M** (2010) Tamoxifen dose response and conditional cell marking: Is there control? *Mol Cell Neurosci* *45*:132-138. Selected scientific image featured on cover (PMID: 20600933).
- Ess, K.C. (2006). The neurobiology of tuberous sclerosis complex. *Semin Pediatr Neurol* *13*, 37-42.

- Hagan N, **Zervas M** (2011) *Wnt1* expression temporally allocates upper rhombic lip progenitors and defines their terminal cell fate in the cerebellum. *Mol Cell Neurosci* 49:217-229. PMID: 22173107 (manual entry for PMCID, ID pending).
- Hentges, K.E., Sirry, B., Gingeras, A.C., Sarbassov, D., Sonenberg, N., Sabatini, D., and Peterson, A.S. (2001). FRAP/mTOR is required for proliferation and patterning during embryonic development in the mouse. *Proc Natl Acad Sci U S A* 98, 13796-13801.
- Landisman, C.E., and Connors, B.W. (2007). VPM and PoM nuclei of the rat somatosensory thalamus: intrinsic neuronal properties and corticothalamic feedback. *Cereb Cortex* 17, 2853-2865.
- Madisen, L., Zwingman, T.A., Sunkin, S.M., Oh, S.W., Zariwala, H.A., Gu, H., Ng, L.L., Palmiter, R.D., Hawrylycz, M.J., Jones, A.R., Lein, E.S., and Zeng, H. (2010). A robust and high-throughput Cre reporting and characterization system for the whole mouse brain. *Nat Neurosci* 13, 133-140.
- Meyer, H.S., Wimmer, V.C., Oberlaender, M., de Kock, C.P., Sakmann, B., and Helmstaedter, M. (2010). Number and laminar distribution of neurons in a thalamocortical projection column of rat vibrissal cortex. *Cereb Cortex* 20, 2277-2286.
- Normand E, Browning C, Machan JT, **Zervas M** (2012) Seizures and compulsive grooming behaviors resulting from thalamus-specific *Tsc1* gene inactivation. *Nature Medicine*. Manuscript #NMED-A60580, Submitted.
- Normand E, Browning C, Hagan N, **Zervas M** (2012) Genetic marking of neural circuits. *Gene Exp Patterns*, Submitted.
- Ridler, K., Bullmore, E.T., De Vries, P.J., Suckling, J., Barker, G.J., Meara, S.J., Williams, S.C., and Bolton, P.F. (2001). Widespread anatomical abnormalities of grey and white matter structure in tuberous sclerosis. *Psychol Med* 31, 1437-1446.
- Swiech, L., Perycz, M., Malik, A., and Jaworski, J. (2008). Role of mTOR in physiology and pathology of the nervous system. *Biochim Biophys Acta* 1784, 116-132.
- Zervas, M.**, Millet, S., Ahn, S., and Joyner, A.L. (2004). Cell behaviors and genetic lineages of the mesencephalon and rhombomere 1. *Neuron* 43, 345-357.

Delineating a temporal window of *Tsc1* requirement for proper brain development and function

Elizabeth Normand¹, Catherine Browning², Jason T. Machan³, and Mark Zervas²

¹Department of Neuroscience, Division of Biology and Medicine, Brown University, 70 Ship St., Providence, RI 02903

²Department of Molecular Biology, Cell Biology and Biochemistry, Division of Biology and Medicine, Brown University, 70 Ship St., Providence, RI 02903

³Departments of Orthopedics and Surgery at Rhode Island Hospital and the Warren Alpert Medical School at Brown University, Providence, Rhode Island 02903

Correspondence should be addressed to M.Z. (mark_zervas@brown.edu)

Address:

Laboratory of Developmental Neurobiology, Genetics and Neurological Disease

Department of Molecular Biology, Cell Biology and Biochemistry

Division of Biology and Medicine

Box G-E436

Brown University

Providence, RI 02912

Courier delivery:

Laboratories for Molecular Medicine

70 Ship Street, Rm. 436

Providence, RI 02903

Email: Mark_Zervas@brown.edu

Tel: 401-863-6840

Fax: 401-863-9653

Web page: http://research.brown.edu/myresearch/Mark_Zervas

Running title: *Tsc1* inactivation in the developing thalamus

Key words: Tuberous Sclerosis, mTOR, thalamus, neurodevelopment, neuron size, seizures, repetitive grooming.

ABSTRACT

Tuberous Sclerosis is a developmental genetic disorder caused by mutations in *TSC1* with significant incidence of epilepsy, autism, and cognitive disability. Studies into the cause of these neurological deficits have focused on the neocortex, but studies suggest the thalamus may also be affected in Tuberous Sclerosis. We hypothesized that the deletion of *Tsc1* at specific developmental stages differentially affects thalamic architecture and causes distinct behavioral phenotypes. Therefore, we deleted the murine *Tsc1* gene within the developing thalamus with temporal control and analyzed the cellular and behavioral consequences. We show that *Tsc1* inactivation in the immature thalamus alters thalamic architecture and causes seizures and compulsive grooming behaviors in adult mice. Interestingly, when we inactivate thalamic *Tsc1* at a later embryonic stage, the behavioral phenotypes are averted. Collectively, we demonstrate that abnormalities in a discrete population of subcortical neurons during a critical developmental period are sufficient to cause global brain dysfunction.

INTRODUCTION

Tuberous Sclerosis (TS) is a complex mosaic genetic disorder that affects one in 6000 children¹. This disease commonly presents in infancy or early childhood and has been diagnosed at 20 weeks of gestation², suggesting an early developmental basis for the disease. Though TS is characterized by benign tumor-like growths (hamartomas) in multiple organs, neurological involvement is also extremely common and quite debilitating. Many patients experience cognitive impairment (45%)³, sleep disturbances (58%)^{4,5}, seizures (85%)⁶ and/or autism (20-50%)⁷. Previously, it was thought that hamartomas in the brain were the cause of the neurological symptoms⁸. However, it has been shown that the extent of hamartomas does not necessarily correlate with the severity of neurological impairment^{9,10}. This finding suggests that more subtle, still unresolved, aspects of brain development or function are perturbed in TS.

Many studies on *Tsc* loss-of-function within the brain have primarily emphasized the effects on neurons of the cerebral cortex¹¹. Subcortical regions have not been extensively evaluated thus far, although one important subcortical brain structure that warrants investigation based on human imaging studies is the thalamus. MRI-imaging studies of patients with TS show significantly decreased thalamic gray matter volume that correlates with poor performance on memory tasks¹². Thalamic involvement in TS is interesting because the thalamus plays a crucial role in higher order cognitive processes^{13,14} and provides the majority of sensory inputs to the cortex. In addition to its extensive reciprocal cortical connectivity, the thalamus also projects heavily to the striatum as part of the thalamostriatal information loop. This circuitry is thought to regulate attentional switching, and dysfunction of the striatum has been implicated in obsessive compulsive disorder and autism¹⁵⁻¹⁷. The thalamus has also been reported to play a role in seizures and sleep patterns^{18,19}. Perturbation of thalamic function therefore has the potential to impair normal cognitive processing by providing aberrant regulation of the neocortex and the striatum. Thus, the thalamus is a compelling brain region to investigate for involvement in TS.

Genetically, TS is caused by mutations in either of two tumor suppressor genes, *TSC1*²⁰ or *TSC2*²¹, and is inherited in an autosomal dominant manner. In addition to the inherited mutation, a second somatic mutation in the remaining functional allele results in loss of heterozygosity and gives rise to isolated *TSC*-null cells that may proliferate and contribute to the formation of hamartomas²². This “two-hit” mechanism, common to cancer disorders, effectively results in a mosaic population of cells in a patient’s organs: a discrete population that has undergone a second hit to become null for *TSC1* or *TSC2*, and surrounding cells that remain heterozygous for *TSC1* or *TSC2*. However, it is unclear whether this two-hit

mechanism underlies the neurocognitive aspects of TS²³⁻²⁵. To experimentally emulate this mosaic state within the brain and test whether limited mosaicism can disrupt global brain function, we employed an inducible CreER/*loxP*-based method in mice²⁶, which produces a spatially discrete, mosaic population of *Tsc1*-mutant cells surrounded by unaffected cells.

Molecularly, the protein products of the *TSC1* and *TSC2* genes interact to form a heterodimer that negatively regulates mTOR. The mTOR pathway, in turn, modulates a wide array of important cellular processes²⁷. During brain development, tissue patterning, cell fate specification, cell growth, differentiation, and axonal connectivity are tightly regulated to establish proper brain architecture and function²⁷. The multifaceted nature of the mTOR pathway raises the possibility that the effects of *TSC* loss-of-function varies depending on a particular cell's identity, function, or developmental state at the time of *TSC* mutation. Thus, controlling the spatial and temporal deletion of *Tsc1* in targeted cell types and analyzing the resulting phenotypes will advance our understanding of this complex disease. Because our CreER/*loxP* experimental system is temporally inducible, we are able to temporally target *Tsc1* inactivation to distinct timepoints during brain development. This experimental approach has allowed us to begin to parse apart the dynamic developmental requirements for functional *Tsc1*.

RESULTS

Temporal contribution of the *Gbx2* lineage to adult thalamic neurons

To temporally and spatially control *Tsc1* gene deletion, we combined three genetically-modified mouse alleles (Supplemental Fig. 1): *Gbx2*^{CreER}, which limits CreER expression to thalamic cells²⁸; *Tsc1*^{fl}, which is converted into a null allele (*Tsc1*^Δ) by Cre-mediated recombination²⁹ (Supplemental Fig. 2); and one of two conditional reporter genes (*R26R*³⁰ or *R26tdTomato*³¹), both of which are activated by Cre-mediated recombination to constitutively produce β-galactosidase (β-gal) or red fluorescent protein (RFP), respectively. Although CreER activation by tamoxifen is transient (approximately 30 hours), recombination produces permanent inactivation of the *Tsc1* gene (*Tsc1*^Δ) (Fig. 1) and permanent activation of the reporter allele (Supplemental Fig. 1b). Hereafter, *Gbx2*^{CreER}-mediated conversion of the *Tsc1*^{fl} allele into the *Tsc1*^Δ allele within the thalamus will be referred to as *Tsc1*^{Δthal}.

We first characterized the extent, spatial distribution, and identity of neurons that underwent *Gbx2*^{CreER}-mediated recombination in order to determine which neurons would be affected by *Tsc1* conditional deletion in subsequent experiments. We performed genetic inducible fate mapping³³ by administering tamoxifen to pregnant females carrying *Gbx2*^{CreER}; *R26R* embryos at embryonic day (E)12.5 or E18.5. Upon reaching adulthood, sagittal brain sections from these animals were analyzed by ICC for β-gal expression. This analysis revealed that E12.5 fate-mapped cells were distributed widely throughout the full extent of the thalamus. In animals that received tamoxifen at E18.5, the overall extent of recombination was lower, especially in more lateral regions of the thalamus (Supplemental Fig. 3). We further investigated whether recombination was preferentially targeted to a particular thalamic cell type by immunostaining for β-gal in combination with parvalbumin (PV) and calbindin. Within relay nuclei such as ventroposteromedial and medial geniculate nuclei, β-gal+ cells contributed to both cell types, although they were conspicuously absent in the PV-expressing thalamic reticular nucleus (Supplemental Fig. 4).

The mTOR pathway rapidly becomes dysregulated after embryonic *Tsc1* deletion.

We inactivated *Tsc1* by administering tamoxifen to E12.5 embryos, when thalamic neurons are transitioning from a proliferative to a differentiated state and are preparing to extend axonal projections

toward the cortex (Fig. 6). We first investigated how quickly thalamic neurons respond to *Tsc1* inactivation by comparing mTOR pathway activity in *Tsc1*^{+/+} and *Tsc1* ^{Δ thal/ Δ thal} embryos 48 hours post-deletion (Fig. 1). For this analysis, we detected phosphorylation of the S6 ribosomal protein at Serine240/244 (p-S6_{Ser240/244}) or Serine 235/236 (p-S6_{Ser235/236}), which are reliable downstream readouts of mTOR pathway activity. We observed basal p-S6_{Ser240/244} expression throughout the wildtype E14.5 embryonic brain (Fig. 1a), consistent with the requirement for mTOR during early development³⁴. Nevertheless, in the E14.5 *Tsc1* ^{Δ thal/ Δ thal} mutants, there was an appreciable increase in thalamic p-S6_{Ser240/244} levels versus controls (Fig. 1a,b). Five days after *Tsc1* deletion, at E17.5, thalamic levels of p-S6_{Ser240/244} were dramatically increased in *Tsc1* ^{Δ thal/ Δ thal} embryos compared to controls (Fig. 1c,d). These experiments show, for the first time, how rapidly neurons respond to *Tsc1* inactivation during embryogenesis. In the adult thalamus, mTOR dysregulation persisted in mature *Tsc1* ^{Δ thal/ Δ thal} neurons and was negligible in the *Tsc1*^{+/+} and *Tsc1*^{+/ Δ thal} thalamus (Fig. 1e-g). Similar results were seen with p-S6_{Ser235/236} at all stages (data not shown). This rapid and sustained cellular response may be an important factor in studies considering the use of mTOR inhibitors.

Early embryonic (E12.5) *Tsc1* deletion produces abnormalities in mature thalamic neurons.

To determine whether thalamic neurons exhibited morphological changes as a result of long-term mTOR dysregulation, we immunolabeled adult brain sections for microtubule-associated protein 2 (MAP-2), a neuronal marker that localizes to the soma and dendrites, and p-S6_{Ser240/244}. To quantify cell size, we manually outlined cell bodies based solely on MAP-2 staining (Fig. 2, panels 1-4). During this process, the red (p-S6_{Ser240/244}) channel was cloaked to blind the observer to the status of mTOR in individual cells. From these outlines, cell areas were calculated. The red channel was then uncloaked to reveal p-S6 levels (Fig. 5a-c). The mosaic nature of CreER-mediated recombination³² resulted in 70% of thalamic neurons undergoing *Tsc1* inactivation (n=3 animals). We took advantage of this mosaicism and sorted neurons into two populations: *Tsc1* ^{Δ / Δ} neurons that expressed high levels of p-S6_{Ser240/244} (Fig. 5c, arrowheads) and *Tsc1*^{fl/fl} neurons that were p-S6_{Ser240/244}-negative (Fig.5c, arrows). Statistical analysis of these populations revealed that the average soma area of *Tsc1* ^{Δ / Δ} thalamic neurons (403 μ m²) was increased over that of *Tsc1*^{+/+}, *Tsc1* ^{Δ /+}, and *Tsc1*^{fl/fl} neurons (220 μ m², 209 μ m², and 203 μ m² respectively), which was statistically significant (p=0.003, Fig. 5d). Because *Tsc1*^{fl/fl} cells that neighbored *Tsc1* ^{Δ / Δ} cells were of normal size, we conclude that cell overgrowth occurs in a cell-autonomous manner.

Because of mTOR's reported role in axon guidance³³, we next investigated whether thalamic projections were affected by *Tsc1* inactivation. For this, we took advantage of the highly organized and reproducible nature of thalamic projections to the cortical whisker barrels³⁴. We used the *R26*^{tdTomato} conditional reporter allele to label the full extent of recombined neurons with RFP, allowing unbiased analysis of thalamic projections^{31,35}. In control animals, thalamocortical axons innervated layer 4 whisker barrels in somatosensory cortex, with synapses located in discrete clusters corresponding to individual whiskers, similar to descriptions from studies using non-genetic labeling methods³⁴. In contrast, *Tsc1* ^{Δ thal/ Δ thal} mice had a noticeably more diffuse pattern of whisker barrel cortical innervation (Fig. 3a,b). Within the internal capsule of the *Tsc1* ^{Δ thal/ Δ thal} brains, thalamocortical axon fascicles also appeared more diffuse and disorganized compared to controls (Fig. 3a,b). We confirmed these findings using an independent approach of lentiviral-GFP infection of adult thalamic relay nuclei in control and mutant animals (Supplemental Fig. 6) In addition to this disorganization, we detected aberrant PV expression in fibers within the internal capsule of *Tsc1* ^{Δ thal/ Δ thal} brains, which was not apparent in *Tsc1*^{+/+} or *Tsc1*^{+/ Δ thal} controls (Fig. 3c-g). From the spatial location of these fibers, the lack of recombination within the nearby PV+ thalamic reticular nucleus, and the presence of PV+/ β -gal+ cell bodies in the thalamic relay nuclei (Fig. 3e,h) we speculated that these fibers were thalamocortical axons that are aberrantly expressed PV.

Because previous TS mouse models have described decreased cortical myelination^{36,37} and increased GFAP+ astrocytes in the hippocampus^{37,38}, we assayed for myelination (MBP) and gliosis (GFAP) in the *Tsc1* ^{Δ thal/ Δ thal} thalamus. Control mice had clear MBP labeling throughout the brain, including within the thalamus and the internal capsule (Fig. 3a). Only sporadic GFAP+ cells were observed, consistent with previous descriptions of GFAP expression in the thalamus³⁹ (Supplemental Fig. 7). Neither MBP nor GFAP labeling differed in *Tsc1* ^{Δ thal/ Δ thal} mutant brains (Fig. 3b and Supplemental Fig. 7). In addition, because neuronal storage disorders have similar findings of enlarged dysmorphic neurons as those seen in TS brains, we assayed thalamic neurons for the presence of GM2 ganglioside, which accumulates in neuronal storage disorders⁴⁰. GM2 staining was not detected in mutant thalamic neurons (data not shown). These results confirmed that thalamic neuron overgrowth in TS was not related to defects in neuronal storage, did not cause reactive gliosis, and that thalamocortical axons were not compromised by myelination defects.

Collectively, our cellular analysis revealed that mature thalamic neurons lacking functional *Tsc1* experienced dramatic mTOR dysregulation, significant overgrowth, aberrant axonal PV expression, and altered thalamocortical axon organization.

Thalamic *Tsc1* deletion at E12.5 causes frequent seizures and overgrooming in adult mice.

Tsc1 ^{Δ thal/ Δ thal} adults and littermate controls that had received tamoxifen at E12.5 were observed in their homecage to determine whether thalamic deletion of *Tsc1* caused overt behavioral changes. At two months of age, *Tsc1* ^{Δ thal/ Δ thal} mice began to develop severe skin lesions (Fig. 4a), while their littermates (*Tsc1*^{+/+}, *Tsc1*^{fl/fl}, or *Tsc1*^{+/ Δ thal}) never showed such lesions (Fig. 4c). Because control littermates never developed lesions, but were housed in the same cage with the lesioned mice, we hypothesized that the lesions in the *Tsc1* ^{Δ thal/ Δ thal} mutants were due to excessive self-grooming, rather than fighting or allogrooming. To confirm this, animals were videotaped for 10-minute periods twice a week in their homecage. A blinded observer scored the amount of time spent grooming by each mouse in the video sessions. A second trainer also evaluated videos screened by the first observer; the observers' tallies showed a high correlation of concordance. In support of our hypothesis that thalamic deletion of *Tsc1* would affect behavior, *Tsc1* ^{Δ thal/ Δ thal} mice spent significantly more time grooming (24.1% of recorded time) than *Tsc1*^{+/+} and *Tsc1*^{+/ Δ thal} mice (3.0% and 3.8% respectively; $p < 0.0001$; $n \geq 11$ mice per genotype) (Fig. 4d). The wounds were differentially located across the population, but each individual tended to preferentially groom a particular region. Importantly, the increase in repetitive excessive grooming was apparent even before wounds developed (Supplemental Video 1), indicating that the wound was not the cause of the grooming, but rather a result of it.

In addition to repetitive grooming behaviors, *Tsc1* ^{Δ thal/ Δ thal} mice exhibited spontaneous and frequent convulsive seizures in their homecage, which were never observed in littermates. The seizure events were highly stereotyped and began with prolonged grooming of the hindlimb, followed by loss of upright posture, then a tonic-clonic state during which the body entered into a convulsive, twisted posture (Fig. 4b, Supplemental Video 1). An observer blinded to genotype quantified the frequency and duration of seizures. The *Tsc1* ^{Δ thal/ Δ thal} mice averaged 3.7 seizures/hour (95%CI = 2.0-6.9 seizures/hour) (Fig. 7e), and these events typically lasted for 10 seconds. Control littermates never exhibited seizures. Ten of the eleven *Tsc1* ^{Δ thal/ Δ thal} mice that were analyzed (91%) experienced seizures as described above during the recording sessions. In contrast, the 11th mouse did not have overt seizures, but displayed abnormal behavior in that it remained in a motionless, sleep-like state for minutes at a time (Supplementary Video 2). Thus, we conclude that 100% of *Tsc1* ^{Δ thal/ Δ thal} mice displayed abnormal behavior, with occasional variations in form and severity. Notably, the extent of grooming and the frequency of seizures were not correlated.

Late embryonic deletion of *Tsc1* at E18.5 dysregulates mTOR, but does not elicit widespread behavioral changes in adult mice.

To further parse apart the developmental requirement for *Tsc1*, we also administered tamoxifen just before birth, at E18.5. These experiments allowed us to compare the effects of *Tsc1* inactivation within the same brain structure, but at two distinct developmental stages. E18.5 embryos received tamoxifen and, upon reaching adulthood, were analyzed for mTOR pathway activity and for cell size. Our analysis demonstrated that mTOR was dysregulated in thalamic neurons, as evidenced by increased pS6₂₄₀, similar to *Tsc1* deletion at E12.5 (Fig. 5a,b). There was also a qualitative increase in neuronal size in these animals, similar to the E12.5 inactivation experiments (Fig. 5c,d). However, while the size increase was similar, fewer thalamic neurons were affected by the E18.5 deletion compared to the E12.5 *Tsc1* ^{Δ thal/ Δ thal} experiments. Behaviorally, mice with *Tsc1* inactivation at E18.5 appeared normal and, even by 5 months of age, still did not show any signs of developing the characteristic wounds from overgrooming (Fig. 5). Of 17 *Tsc1* ^{Δ thal/ Δ thal} mice, we observed only two instances of seizures during weekly observations. Specifically, at 5 months of age a single seizure was elicited in two *Tsc1* ^{Δ thal/ Δ thal} mice upon handling by the experimenters. Notably, this was an age where 91% of E12.5 *Tsc1* ^{Δ thal/ Δ thal} mice had already experienced frequent spontaneous seizures for 3 months.

DISCUSSION

The TSC/mTOR pathway is a multifaceted and complex signaling hub that integrates major signaling pathways and regulates numerous critical cellular functions²⁷. We hypothesized that disrupting the mTOR pathway would elicit different phenotypes depending on the identity and developmental state of the cells in which *Tsc1* was deleted. To test this hypothesis, we developed a mouse model that mimics salient features of TS using CreER/*loxP*-based temporal control of cell-type specific deletion of *Tsc1*. Our initial experiments focused on mutating E12.5 thalamic neurons, which are transitioning from a proliferative to a differentiated state⁴¹. Remarkably, these *Tsc1* ^{Δ thal/ Δ thal} mice exhibit frequent spontaneous seizures despite the fact that the vast majority of neurons in the brain remain genetically normal. Previous studies describing *Tsc1* loss-of-function within different cell types of the mouse brain have also reported seizures in mutant mice. For example, the same *Tsc1*^{*fl/fl*} allele was combined with *hGFAP*^{*Cre*} with the goal of driving recombination in astrocytes and 6/6 of these mice experienced seizures beginning at 2 months of age, with an average frequency of 0.6 seizures/hour⁴². However, *hGFAP*^{*Cre*} also mediates recombination in neuronal progenitors⁴³, suggesting that *hGFAP*^{*Cre*}-mediated deletion of *Tsc1* affected both neurons and astrocytes in these mice. An additional study used the *Tsc1*^{*fl/fl*} allele in concert with *Syn*^{*Cre*} to mediate recombination within post-mitotic neurons of the forebrain beginning at E12.5⁴⁴. Interestingly, only 10% of the *Syn*^{*Cre*};*Tsc1*^{*fl/fl*} mice exhibit seizures and these were only elicited upon handling. In comparison to these studies, 91% of our mice with thalamic deletion of *Tsc1* at E12.5 exhibited frequent spontaneous seizures beginning at 2 months of age. The fact that we observed a severe phenotype despite a more limited population of mutant cells in other studies suggests that perturbing a single node of the thalamocortical or thalamostriatal circuit is more deleterious than widespread mTOR dysregulation. This concept is particularly striking in light of the mosaic nature of TS in humans.

Ours is the first description of a repetitive grooming phenotype related to either *Tsc1* or *Tsc2* deletion. Interestingly, a similar behavioral phenotype is observed in mice with genetic mutations in *Slitrk5*, *Shank3* or *Sapap3*, which are highly expressed in a thalamic target, the striatum⁴⁵⁻⁴⁷. Notably, these well-accepted models of obsessive compulsive disorder and autism, in which the corticostriatal circuit is disrupted, do not have seizures. Our mouse model lacks recombination in the cerebral cortex and has only very sparse striatal recombination (Supplemental Fig. 5). Thus, our findings suggest that the

repetitive behaviors and seizures in our mice may be particularly related to the thalamostriatal or the thalamocortical pathways, respectively. To our knowledge, this is the first TS animal model to exhibit both seizures and repetitive behaviors, suggesting that further study of the role of subcortical circuits in neurocognitive aspects of TS is warranted. This is important because neurological involvement in TS patients is not limited to seizures and may include cognitive deficits and autistic features.

We took advantage of our temporally-inducible experimental system to inactivate thalamic *Tsc1* at an advanced embryonic stage, E18.5, and compared the resulting phenotypes to the earlier E12.5 deletion. By E18.5, thalamic neurons have fully differentiated, extended their axons into the cortex, and initiated synapse formation with cortical targets⁴⁸ (Fig. 6). However, thalamic neurons with *Tsc1* deletion at E18.5 still experience dysregulated mTOR and overgrowth compared to controls. Interestingly, thalamic deletion of *Tsc1* at E18.5 failed to produce the behavioral phenotypes seen in the E12.5 inactivation experiments. A recent study showed that postnatal treatment with rapamycin, which inhibits mTOR activity, causes cell size to return to normal and prevents seizures³⁶. Thus, we conjectured that increased cell size (and the putative effects on electrical properties of the mutant neurons) could be the underlying cause of seizures. However, the fact that we also see increased cell size in the E18.5 experiments, but without spontaneous seizures, argues against this possibility. The most likely explanation is that by inactivating *Tsc1* just before birth, thalamic axon pathfinding was able to proceed normally prior to recombination, resulting in relatively normal thalamic circuits (Fig. 6). We expect that postnatal development processes, such as synapse formation and maintenance, could be affected in both experiments. This is presumably why two of the seventeen E18.5-deletion animals experienced a seizure, although they were not spontaneous seizures. While the developmental explanation is the most likely, the diminished behavioral findings in the E18.5 animals could simply be due to the decreased extent of recombination at E18.5, either because fewer thalamic cells are affected overall (Supplemental Fig. 2), or because some thalamic relay nuclei are spared due to dynamic *Gbx2*^{CreER} expression patterns²⁸. This would indicate that there is a critical threshold for mutant cells in the brain, above which the normal cells can no longer compensate, and behavioral abnormalities arise.

Here we have described the first use of an inducible CreER/*loxP* genetic system to investigate the consequences of mTOR dysregulation in the developing thalamus. We have exploited the inducible nature of this system to begin to interrogate the requirement for *Tsc1* function at different developmental timepoints within the thalamus. Our current experiments have shown that thalamic neurons lacking *Tsc1* function from E12.5 rapidly undergo mTOR dysregulation, experience neuronal overgrowth, and display axonal abnormalities. Furthermore, these animals, which lack *Tsc1* function in 70% of thalamic neurons, experience frequent spontaneous seizures and exhibit injurious repetitive motor behaviors. In comparison, animals lacking thalamic *Tsc1* beginning at E18.5 also exhibit dysregulated mTOR and increased cell size, but have normal grooming behavior and only rare seizures upon handling. Thus, we have demonstrated a putative window of development during which *Tsc1* mutations and mTOR dysregulation in a single subcortical node can lead to epilepsy and repetitive grooming behaviors. These findings provide an important starting point from which to further dissect the dynamic nature of mTOR function in brain development.

ACKNOWLEDGEMENTS

We thank members of the Brown Neuroscience community for their helpful comments. This work was supported in part by a Brown Institute for Brain Science Research Award (EN), the National Institutes of Health Neuroscience Graduate Student Training grant (NS062443-02, EN), a Department of Defense Congressionally-Directed Medical Research Program award (TS100067, MZ) and startup funds (MZ). We also thank Dr. Scott Cruikshank for his help with the lentiviral experiments.

AUTHOR CONTRIBUTIONS

M.Z. and E.N. wrote the manuscript and designed the experiments. E.N. performed the experiments and analyzed the cellular data. E.N. and C.B. analyzed the behavioral data. J.T.M. performed statistical analysis.

FIGURE LEGENDS

Figure 1. Conditional deletion of *Tsc1* within developing thalamus results in mTOR pathway dysregulation within 2-5 days that persists into adulthood. E12.5 embryos were exposed to tamoxifen to induce *Gbx2*^{CreER}-mediated recombination of the *Tsc1*^{fl} allele. Embryos were subsequently harvested at E14.5 (a-b), E17.5 (c-d), or adulthood (e-g) and ICC was performed to detect p-S6_{Ser240/244} levels (red) in thalamic cells of control (*Tsc1*^{+/+}, *Tsc1*^{fl/fl}) or mutant (*Tsc1*^{Δthal/Δthal}) animals. Comparison of p-S6 levels revealed a slight increase in p-S6 expression 2 days after *Tsc1* inactivation (a versus b) and a robust increase in p-S6 levels 5 days after inactivation (c versus d). In the mature thalamus, p-S6_{Ser240/244} levels were negligible in both wildtype and heterozygous controls (e,f) but are high in *Tsc1*^{Δthal/Δthal} mutants (g). Similar results were seen for the p-S6_{Ser235/236} epitope (data not shown). n≥3 animals per genotype per stage. Scale bars: (a,b) 30μm, (c,d) 15μm, (e-g) 30μm.

Figure 2. *Tsc1* deletion at E12.5 causes overgrowth in mature thalamic neurons. (a-c) *Tsc1*^{+/+}, *Tsc1*^{+/Δthal}, or *Tsc1*^{Δthal/Δthal} embryos received tamoxifen at E12.5. Upon reaching adulthood, ICC was performed for MAP-2 (green) and p-S6_{Ser240/244} (red). Hoechst nuclear counterstain is blue. The red channel was cloaked and soma boundaries were manually outlined based solely on MAP-2 labeling using Velocity software (panels 1-4). After area measurements were taken, the red (p-S6_{Ser240/244}) channel was revealed and cells were sorted into p-S6-positive (red) and p-S6-negative (green) populations. 70% (621/878) of measured neurons in the *Tsc1*^{Δthal/Δthal} thalamus underwent recombination, based on p-S6 levels. (d) The soma area of each cell was plotted on a log scale with the geometric mean indicated by a horizontal line. The geometric means and 95% confidence intervals were: *Tsc1*^{+/+}: 220.0μm (95%CI 211.7μm-228.6μm); *Tsc1*^{+/Δthal}: 209.5μm (201.6μm-217.7μm); *Tsc1*^{Δthal/Δthal}, grey: 220.3μm (95%CI 188.5μm-220.2μm); *Tsc1*^{Δthal/Δthal}, black: 424.2μm (95%CI 383.8μm-424.4μm). Comparing populations with the Holm test confirms that *Tsc1*^{fl/fl} neurons (grey) are not statistically different than *Tsc1*^{+/+} or *Tsc1*^{+/Δthal} cells (p=0.303), while *Tsc1*^{Δthal/Δthal} cells (black) are significantly larger than p-S6 negative neurons (grey, *p=0.003, **p=0.004). Number of cells measured per population (summed across 3 animals/genotype) is indicated on the graph. Scale bars: 16μm (a-c), 22μm (1-4).

Figure 3. *Tsc1*^{Δthal/Δthal} mutants have abnormal thalamic circuits. Tamoxifen was administered at E12.5 to induce recombination of the *Tsc1*^{fl} allele. (a-b) ICC was performed to detect MBP (green) and the *tdTomato* reporter protein, RFP (red). MBP levels did not differ between controls and mutants. RFP+

thalamocortical innervation of whisker barrels was highly organized and discrete in control animals (a1), but is more diffuse in $Tsc1^{\Delta thal/\Delta thal}$ mutants, where individual barrels were less apparent (b1). Within the internal capsule of $Tsc1^{\Delta thal/\Delta thal}$ brains, thalamic axon bundles were also less sharply defined (b2). (c-h) ICC was performed for parvalbumin (PV, red) and β -gal (green). Hoechst 33342 nuclear counterstain, blue. (c,f) PV staining can be seen lateral to the thalamus, within the internal capsule, and in the external capsule (white arrows) of $Tsc1^{\Delta thal/\Delta thal}$ brains (f), but was absent in $Tsc1^{+/ \Delta thal}$ or $Tsc1^{+/+}$ control brains (c, data not shown). (d,g) High magnification images from the boxed regions in c,f showed that axon bundles within the internal capsule of the mutant brain contained PV+ fibers (yellow arrowheads) that were not seen in controls (d). Thalamic relay cell bodies were double positive for PV and β -gal (white arrowheads), raising the possibility that the PV fibers originate from PV-expressing $Tsc1^{\Delta/\Delta}$ relay cells. Scale bars: 240mm (a,b); 61um (a1,2 and b1,2); 180 μ m (c,f); 30 μ m (d,g); 15um (e,h). thal, thalamus; str, striatum; ctx, cerebral cortex.

Figure 4. $Tsc1^{\Delta thal/\Delta thal}$ mice exhibit abnormal grooming behavior and frequent seizures subsequent to $Tsc1$ inactivation at E12.5. (a) At approximately 2 months of age, $Tsc1^{\Delta thal/\Delta thal}$ mice began to exhibit excessive grooming behaviors that often resulted in lesions, as pictured. (b) $Tsc1^{\Delta thal/\Delta thal}$ mice also exhibited convulsive seizures, characterized by twisting of the body and loss of upright posture. (c) An unaffected wild-type mouse is shown for comparison. (d) Grooming behavior was quantified and compared across genotypes. Average percent of time spent grooming for each mouse was plotted, with the pooled average for each genotype indicated by the horizontal bar: $Tsc1^{+/+}$: mean 3.0% (95%CI 2.4-3.9%), $Tsc1^{+/ \Delta thal}$: mean 3.8% (95%CI 3.0-4.9%), $Tsc1^{\Delta thal/\Delta thal}$: mean 24.1% (95%CI 21.8-26.5%). (e) The frequency of seizures per hour was quantified. Each individual's average seizure frequency was plotted, with the pooled average for each genotype indicated by the horizontal bar ($Tsc1^{+/+}$ and $Tsc1^{+/ \Delta thal}$ population geometric means are 0 seizures/hr; $Tsc1^{\Delta thal/\Delta thal}$ geometric mean: 3.7 seizures/hr (95%CI 2.0-6.9seizures/hr).

Figure 5. Late embryonic deletion of $Tsc1$ in the thalamus produces cellular abnormalities, but virtually normal behavior. (a-d) Sagittal brain sections from controls and $Tsc1^{\Delta thal/\Delta thal}$ mutant mice that received tamoxifen at E18.5 were immunostained for MAP-2 (green) and p-S6_{Ser240/244} (red). (a,b) Low magnification images show mTOR pathway dysregulation throughout the $Tsc1^{\Delta thal/\Delta thal}$ thalamus. (c,d) High magnification images show that soma size (based on MAP-2 staining) was larger in $Tsc1^{\Delta thal/\Delta thal}$ thalamic neurons. (e-g) $Tsc1^{\Delta thal/\Delta thal}$ mice did not develop wounds from overgrooming by 6 months of age. At approximately 5 month of age, 2 of the 17 $Tsc1^{\Delta thal/\Delta thal}$ mice exhibited a seizure that was induced upon handling, while the remaining 15 mice never had a seizure during any of the observation sessions, even upon handling.

Figure 6. A developmental time window during which $Tsc1$ inactivation causes behavioral phenotypes. Stages of thalamic developmental stages are shown in relation to mouse age. Inactivation of thalamic $Tsc1$ from E12.5 through adulthood (spotted region) causes spontaneous seizures and repetitive overgrooming in $Tsc1^{\Delta thal/\Delta thal}$ mice. In contrast, inactivation of thalamic $Tsc1$ from E18.onward, when neuronal differentiation and axon pathfinding processes are complete, does not cause spontaneous seizures or grooming abnormalities.

MATERIALS AND METHODS.

Mice. $Tsc1^{fl}$ mice were obtained from Jackson laboratories (stock#005680). $Gbx2^{CreER}$ mice²⁹ and $Rosa26$ reporter ($R26R$) mice³¹ were generously provided by J. Li (UConn Helath Center) and P. Soriano (Mt.

Sinai School of Medicine, respectively. Mice were housed and handled in accordance with Brown University Institutional Animal Care and Use Committee guidelines.

Mouse Breeding and Genotyping. *Gbx2^{CreER}* mice were bred with *R26R* and *Tsc1^{fl/fl}* mice to maintain a compound line. *Gbx2^{CreER};R26R;Tsc1^{fl/+}* males were then bred with *Tsc1^{+/+}*, *Tsc1^{fl/+}*, or *Tsc1^{fl/fl}* females. Genotyping was performed as previously described for the *CreER* and *R26R* alleles⁴⁷. Genotyping for the *Tsc1⁺*, *Tsc1^{fl}*, and *Tsc1^Δ* allele was performed as previously described⁴⁸.

***Tsc1^{fl}* Inactivation and Fate Mapping.** *Tsc1^{fl}* inactivation experiments were conducted by crossing *Gbx2^{CreER};R26R;Tsc1^{fl/+}* males with *Tsc1^{fl/+}* females. The morning (0900) of the day a vaginal plug was detected was designated as 0.5 days post-coitus. 4mg of tamoxifen (20mg/mL in corn oil) was administered by oral gavage⁴⁹ to the timed-pregnant females harboring embryos at embryonic stage (E)12.5 or E18.5 to simultaneously activate the *R26R* allele and induce recombination of the *Tsc1^{fl}* allele into the *Tsc1^Δ* allele (Supplemental Fig. 1).

Tissue Processing and Immunocytochemistry (ICC). For embryonic analysis, timed-pregnant females harboring embryos at the desired pregnancy stage (E14.5 or E17.5) (n≥3 each stage and genotype) were sacrificed at 0900 and the uterine chain was dissected out. Individual embryos were dissected, processed, and sectioned sagittally for ICC analysis as previously described⁴⁷.

For postnatal tissue analysis, pups were weaned at postnatal day (P)21 and genotyped as described above. At P30-35, animals were deeply anesthetized with Nembutal (5mg) and intracardially perfused. Craniotomies were performed as previously described⁴⁹. Brains were embedded in 3.5% agarose and sectioned at a sagittal angle (40 μm) or a thalamocortical angle³⁷ (60 μm) using a Leica vibratome.

Embryonic sections and adult free-floating sections were matched based on morphology, then processed for immunocytochemistry (ICC) by standard methods⁴⁷ using primary antibodies raised against the following antigens: phosphorylated S6 ribosomal protein at Ser240/244 (p-S6_{Ser240/244}, 1:800, Cell Signaling), phosphorylated S6 ribosomal protein at Ser235/236 (p-S6_{Ser235/236}, 1:100, Cell Signaling), β-galactosidase (1:500, Biogenesis), GFP (1:500, Nacalai Tesque or 1:600, Invitrogen), RFP (1:1000, VWR), myelin basic protein (MBP, 1:500, Millipore), MAP-2 (1:500, Sigma), calbindin D-28K (1:1000, Swant), and parvalbumin (1:1000, Sigma). The following secondary antibodies from Invitrogen were used at a 1:500 dilution in 1% normal donkey serum in PBT: Alexa 488 donkey anti-rabbit IgG, Alexa 555 donkey anti-rabbit IgG, Alexa 488 donkey anti-rat IgG, Alexa 555 donkey anti-goat IgG, and Alexa 488 donkey anti-mouse IgG (Molecular Probes). All sections were counter stained using the nuclear marker Hoechst 33342 (Molecular Probes) and mounted on FisherBrand ColorFrostPlus slides using FluoromountG mounting media (Southern Biotech).

Microscopy and Cell Size Analysis. Sections were imaged on a Leica DM600B epifluorescent microscope with Volocity 5.1 imaging software (Improvision). Red, green, and blue channels were imaged separately and pseudocolored as part of the acquisition palettes. Identical exposure settings were used across the three genotypes to allow for direct comparison of labeling intensity.

For cell size analysis, free-floating adult sagittal sections from *Tsc1^{+/+}*, *Tsc1^{fl/+}* and *Tsc1^{fl/fl}* animals (n=3 each genotype) were processed for ICC using primary antibodies to MAP-2 and to phosphorylated S6, as described above. Five thalamic regions (dorsal, ventral, anterior, posterior, and center) from five medial-to-lateral brain levels were imaged at 40x magnification. After the red channel was cloaked to blind the observer to p-S6 levels, the green MAP-2 signal was used to manually outline the edges of clearly

labeled neuronal cell bodies using Velocity's Freehand Tool. The Measure function was used to calculate the perimeter and area of all outlined cell bodies and was exported to Microsoft Excel for data analysis. After analysis, the red p-S6 channel was unmasked in order to sort cells into "p-S6 positive" and "p-S6 negative" cohorts, based on p-S6 immunolabeling intensity. Numbers of measured cells per cohort are indicated in Fig. 2d.

Behavioral Analysis. E12.5 inactivation experiments: $Tsc1^{\Delta thal/\Delta thal}$ mice (n=11) and their littermate controls ($Tsc1^{+/+}$ or $Tsc1^{fl/fl}$, n=19; $Tsc1^{+/\Delta thal}$ n=17) were videotaped in their home cage using a digital camera for 8-minute epochs 2-3 times per week between 2 months of age and 8 months of age. Two $Tsc1^{\Delta thal/\Delta thal}$ mice died prematurely and were not included in the behavioral analysis. Videos were analyzed by an observer who was blinded to animal genotypes. Number and duration of all seizures and self-grooming behaviors were recorded (grooming events lasting less than 1 second were rounded up to 1 second duration). Animals were euthanized for humane reasons when they developed severe grooming lesions. Data was analyzed in Excel (Microsoft) and plotted using KaleidaGraph (Synergy). E18.5 inactivation experiments: $Tsc1^{\Delta thal/\Delta thal}$ mice (n=17) and their littermate controls ($Tsc1^{+/+}$ or $Tsc1^{fl/fl}$, n=19; $Tsc1^{+/\Delta thal}$, n=7) were observed once per week for 8 minutes, beginning at 2 months of age and continuing through 6 months of age by an observer who was blinded to animal genotypes.

Statistics. Generalized Estimating Equations were used to compare genotypes with regards to neuronal size (log-normal generalized model), percent minutes grooming (binomial generalized model grooming/total minutes), percent minutes seizing (binomial generalized model seizure/total minutes), and seizure event rates (negative-binomial generalized model offset by log total hours). For neuronal size, each mouse had multiple cells, which were treated as having correlated error. Cells were divided into those expressing p-S6 and those not expressing p-S6. The former were only present in the knock-out animals, making the comparison between sizes of p-S6 expressing cells and p-S6-negative cells within the knock-outs a within-subjects comparison while those between genotypes were between-subjects comparisons. All comparisons in other models represented between-subjects comparisons, with multiple observations within an animal modeled as having correlated error. For all models, pair-wise comparisons were made using orthogonal contrast statements, with p-values adjusted using the Holm test to maintain family-wise alpha at 0.05.

REFERENCES

1. O'Callaghan, F. J., Shiell, A. W., Osborne, J. P. & Martyn, C. N. Prevalence of tuberous sclerosis estimated by capture-recapture analysis. *Lancet* **351**, 1490 (1998).
2. Park, S.-H. *et al.* Tuberous sclerosis in a 20-week gestation fetus: immunohistochemical study. *Acta Neuropathol* **94**, 180–186 (1997).
3. Joinson, C. *et al.* Learning disability and epilepsy in an epidemiological sample of individuals with tuberous sclerosis complex. *Psychol Med* **33**, 335–344 (2003).
4. Hunt, A. Development, behaviour and seizures in 300 cases of tuberous sclerosis. *J Intellect Disabil Res* **37 (Pt 1)**, 41–51 (1993).
5. Bruni, O., Cortesi, F., Giannotti, F. & Curatolo, P. Sleep disorders in tuberous sclerosis: a polysomnographic study. *Brain Dev.* **17**, 52–56 (1995).
6. Chu-Shore, C. J., Major, P., Camposano, S., Muzykewicz, D. & Thiele, E. A. The natural history of epilepsy in tuberous sclerosis complex. *Epilepsia* **51**, 1236–1241 (2010).
7. Wong, V. Study of the relationship between tuberous sclerosis complex and autistic disorder. *J. Child Neurol.* **21**, 199–204 (2006).

8. Goodman, M. *et al.* Cortical tuber count: a biomarker indicating neurologic severity of tuberous sclerosis complex. *J. Child Neurol.* **12**, 85–90 (1997).
9. Wong, V. & Khong, P.-L. Tuberous sclerosis complex: correlation of magnetic resonance imaging (MRI) findings with comorbidities. *J. Child Neurol.* **21**, 99–105 (2006).
10. Ridler, K., Suckling, J., Higgins, N., Bolton, P. & Bullmore, E. Standardized whole brain mapping of tubers and subependymal nodules in tuberous sclerosis complex. *J. Child Neurol.* **19**, 658–665 (2004).
11. Ehninger, D., De Vries, P. J. & Silva, A. J. From mTOR to cognition: molecular and cellular mechanisms of cognitive impairments in tuberous sclerosis. *J. Intellectual Disabil Res* **53**, 838–851 (2009).
12. Ridler, K. *et al.* Neuroanatomical Correlates of Memory Deficits in Tuberous Sclerosis Complex. *Cerebral Cortex* **17**, 261–271 (2006).
13. Saalman, Y. B. & Kastner, S. Cognitive and perceptual functions of the visual thalamus. *Neuron* **71**, 209–223 (2011).
14. Minamimoto, T. & Kimura, M. Participation of the thalamic CM-Pf complex in attentional orienting. *Journal of Neurophysiology* **87**, 3090–3101 (2002).
15. Smith, Y., Surmeier, D. J., Redgrave, P. & Kimura, M. Thalamic Contributions to Basal Ganglia-Related Behavioral Switching and Reinforcement. *Journal of Neuroscience* **31**, 16102–16106 (2011).
16. Matsumoto, N., Minamimoto, T., Graybiel, A. M. & Kimura, M. Neurons in the thalamic CM-Pf complex supply striatal neurons with information about behaviorally significant sensory events. *Journal of Neurophysiology* **85**, 960–976 (2001).
17. Graybiel, A. M. & Rauch, S. L. Toward a neurobiology of obsessive-compulsive disorder. *Neuron* **28**, 343–347 (2000).
18. Blumenfeld, H. From Molecules to Networks: Cortical/Subcortical Interactions in the Pathophysiology of Idiopathic Generalized Epilepsy. 1–9 (2003).
19. Crunelli, V. & Hughes, S. W. The slow (Δ). *Nat Neurosci* **13**, 9–17 (2010).
20. Slegtenhorst, M. V. Identification of the Tuberous Sclerosis Gene TSC1 on Chromosome 9q34. *Science* **277**, 805–808 (1997).
21. European Chromosome 16 Tuberous Sclerosis Consortium Identification and characterization of the tuberous sclerosis gene on chromosome 16. *Cell* **75**, 1305–1315 (1993).
22. Au, K. S., Hebert, A. A., Roach, E. S. & Northrup, H. Complete inactivation of the TSC2 gene leads to formation of hamartomas. *Am. J. Hum. Genet.* **65**, 1790–1795 (1999).
23. Jozwiak, J. & Jóźwiak, S. Giant cells: contradiction to two-hit model of tuber formation? *Cell. Mol. Neurobiol.* **27**, 251–261 (2007).
24. Henske, E. P. *et al.* Allelic loss is frequent in tuberous sclerosis kidney lesions but rare in brain lesions. *Am. J. Hum. Genet.* **59**, 400–406 (1996).
25. Sepp, T., Yates, J. R. & Green, A. J. Loss of heterozygosity in tuberous sclerosis hamartomas. *J. Med. Genet.* **33**, 962–964 (1996).
26. Brown, A. *et al.* A practical approach to genetic inducible fate mapping: a visual guide to mark and track cells in vivo. *J. Vis. Exp.* (2009).doi:10.3791/1687
27. Hay, N. Upstream and downstream of mTOR. *Genes & Development* **18**, 1926–1945 (2004).
28. Chen, L., Guo, Q. & Li, J. Y. H. Transcription factor Gbx2 acts cell-nonautonomously to regulate the formation of lineage-restriction boundaries of the thalamus. *Development* **136**, 1317–1326 (2009).
29. Kwiatkowski, D. J. *et al.* A mouse model of TSC1 reveals sex-dependent lethality from liver hemangiomas, and up-regulation of p70S6 kinase activity in Tsc1 null cells. *Human Molecular Genetics* **11**, 525–534 (2002).

30. Soriano, P. Generalized lacZ expression with the ROSA26 Cre reporter strain. *Nat. Genet.* **21**, 70–71 (1999).
31. Madisen, L. *et al.* A robust and high-throughput Cre reporting and characterization system for the whole mouse brain. *Nat Neurosci* **13**, 133–140 (2010).
32. Joyner, A. L. & Zervas, M. Genetic inducible fate mapping in mouse: Establishing genetic lineages and defining genetic neuroanatomy in the nervous system. *Dev. Dyn.* **235**, 2376–2385 (2006).
33. Knox, S. *et al.* Mechanisms of TSC-mediated control of synapse assembly and axon guidance. *PLoS ONE* **2**, e375 (2007).
34. Wimmer, V. C., Bruno, R. M., de Kock, C. P. J., Kuner, T. & Sakmann, B. Dimensions of a projection column and architecture of VPM and POM axons in rat vibrissal cortex. *Cerebral Cortex* **20**, 2265–2276 (2010).
35. Hagan, N. & Zervas, M. Wnt1 expression temporally allocates upper rhombic lip progenitors and defines their terminal cell fate in the cerebellum. *Mol. Cell. Neurosci.* **49**, 217–229 (2012).
36. Meikle, L. *et al.* Response of a Neuronal Model of Tuberous Sclerosis to Mammalian Target of Rapamycin (mTOR) Inhibitors: Effects on mTORC1 and Akt Signaling Lead to Improved Survival and Function. *Journal of Neuroscience* **28**, 5422–5432 (2008).
37. Carson, R. P., Van Nielen, D. L., Winzenburger, P. A. & Ess, K. C. Neuronal and glia abnormalities in Tsc1-deficient forebrain and partial rescue by rapamycin. *Neurobiology of Disease* **45**, 369–380 (2012).
38. Uhlmann, E. J. *et al.* Heterozygosity for the tuberous sclerosis complex (TSC) gene products results in increased astrocyte numbers and decreased p27-Kip1 expression in TSC2+/- cells. *Oncogene* **21**, 4050–4059 (2002).
39. Kálmán, M. & Hajós, F. Distribution of glial fibrillary acidic protein (GFAP)-immunoreactive astrocytes in the rat brain. I. Forebrain. *Exp Brain Res* **78**, 147–163 (1989).
40. Zervas, M., Somers, K. L., Thrall, M. A. & Walkley, S. U. Critical role for glycosphingolipids in Niemann-Pick disease type C. *Curr. Biol.* **11**, 1283–1287 (2001).
41. Angevine, J. B. Time of neuron origin in the diencephalon of the mouse. An autoradiographic study. *J. Comp. Neurol.* **139**, 129–187 (1970).
42. Uhlmann, E. J. *et al.* Astrocyte-specific TSC1 conditional knockout mice exhibit abnormal neuronal organization and seizures. *Ann Neurol.* **52**, 285–296 (2002).
43. Casper, K. B. & McCarthy, K. D. GFAP-positive progenitor cells produce neurons and oligodendrocytes throughout the CNS. *Molecular and Cellular Neuroscience* **31**, 676–684 (2006).
44. Meikle, L. *et al.* A Mouse Model of Tuberous Sclerosis: Neuronal Loss of Tsc1 Causes Dysplastic and Ectopic Neurons, Reduced Myelination, Seizure Activity, and Limited Survival. *Journal of Neuroscience* **27**, 5546–5558 (2007).
45. Peça, J. *et al.* Shank3 mutant mice display autistic-like behaviours and striatal dysfunction. *Nature* **472**, 437–442 (2011).
46. Welch, J. M. *et al.* Cortico-striatal synaptic defects and OCD-like behaviours in Sapap3-mutant mice. *Nature* **448**, 894–900 (2007).
47. Shmelkov, S. V. *et al.* Slitrk5 deficiency impairs corticostriatal circuitry and leads to obsessive-compulsive-like behaviors in mice. *Nature Medicine* **16**, 598–602 (2010).
48. Molnár, Z., Higashi, S. & López-Bendito, G. Choreography of early thalamocortical development. *Cereb. Cortex* **13**, 661–669 (2003).

Figure 1 - Normand, Browning, Machan, Zervas

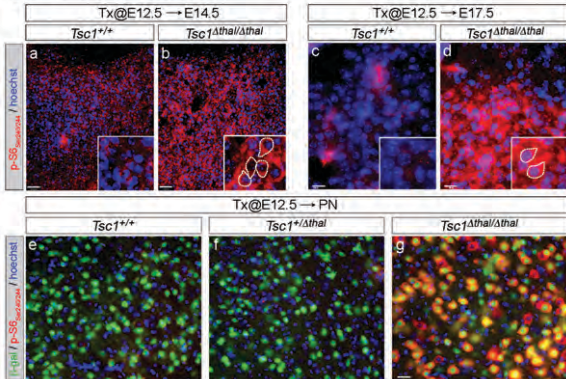


Figure 2 - Normand, Browning, Machan, Zervas

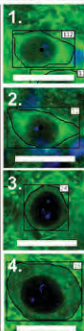
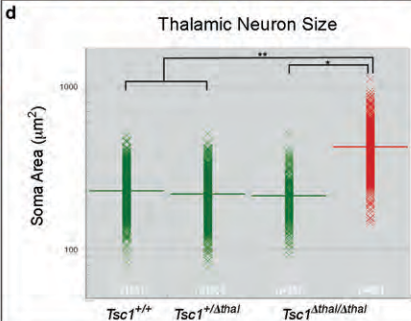
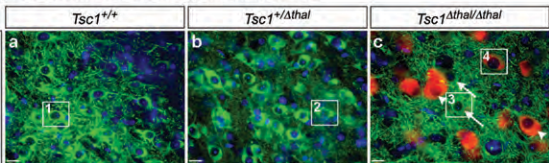


Figure 3 - Normand, Browning, Machan, Zervas

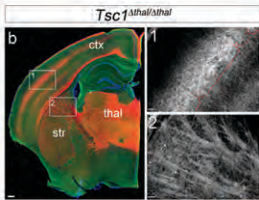
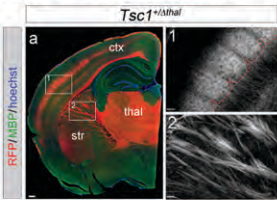


Figure 5 - Normand, Browning, Machan, Zervas

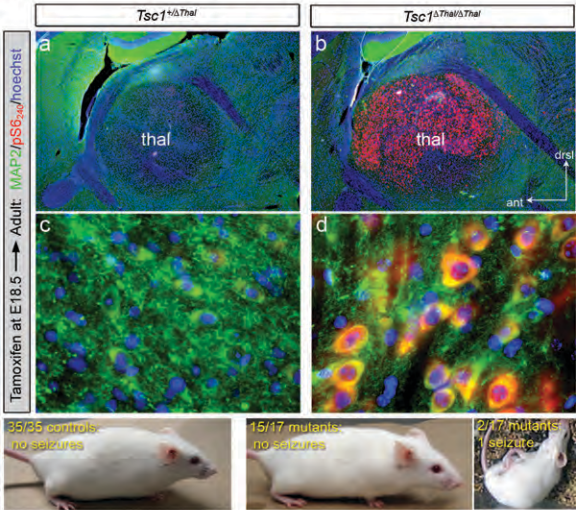
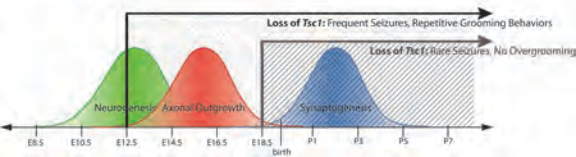


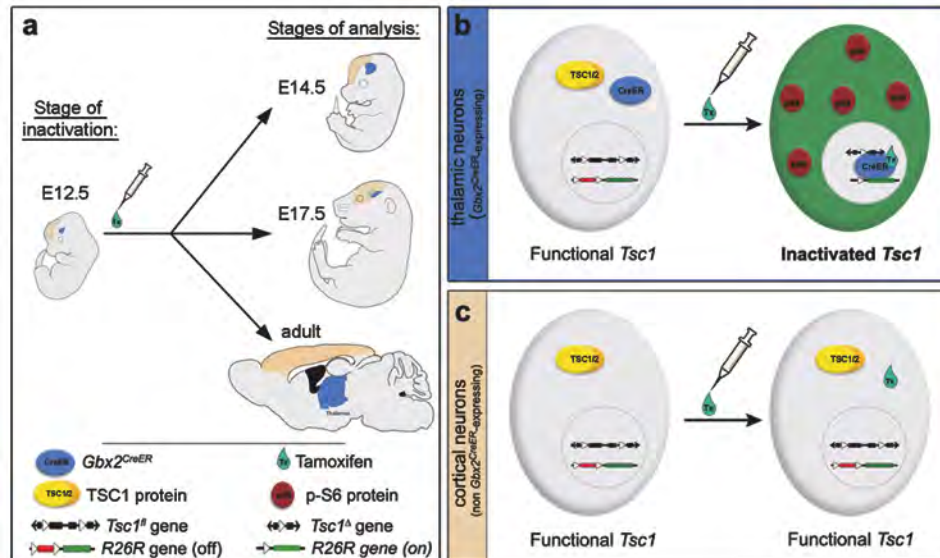
Figure 6 - Normand, Browning, Machan, Zervas



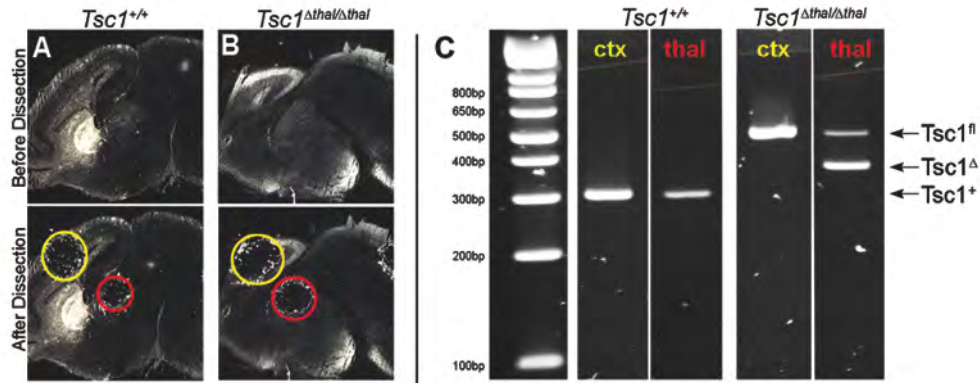
Supplemental Material

Delineating a temporal window of *Tsc1* requirement for proper brain development and function

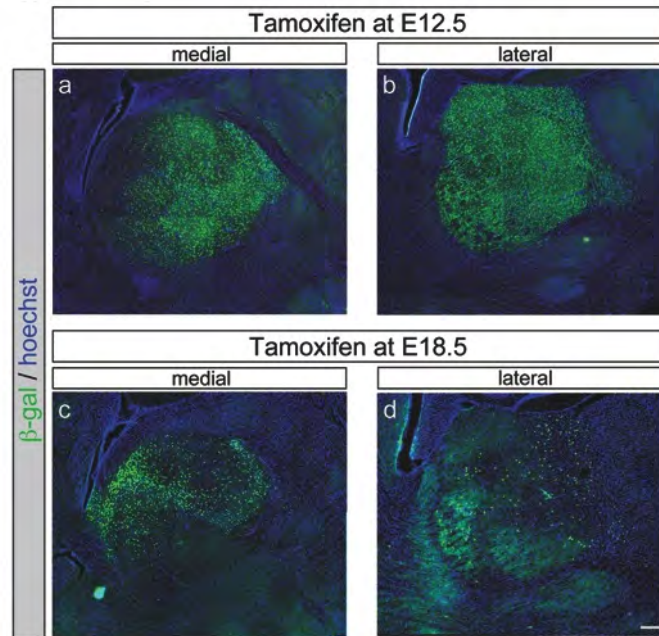
Elizabeth Normand, Catherine Browning, Jason T. Machan, and Mark Zervas



Supplemental Figure 1. Conditional *Tsc1* inactivation strategy. (a) Experimental design is shown. To induce CreER-based recombination of the *Tsc1^f* allele in the thalamus (blue) but not in surrounding brain regions such as the cerebral cortex (tan), tamoxifen is administered to pregnant females harboring E12.5 stage *Gbx2^{CreER}; Tsc1^f* embryos (left). Pups are then analyzed at stage E14.5, E17.5, or adulthood (right) for cellular and behavioral phenotypes. (b, left) A *Gbx2^{CreER}*-expressing neuron in the thalamus possesses the *Tsc1^f* allele and the quiescent *R26R* reporter allele. This cell produces TSC1/2 protein (yellow) as well as CreER protein that is sequestered in the cytoplasm (blue). (b, right) Upon tamoxifen exposure, tamoxifen (aqua) binds to CreER, releasing it from hsp90 binding (not shown) and allowing it to translocate the nucleus. Once in the nucleus, CreER mediates recombination of *loxP* sites (white triangles), leading to conversion of the *Tsc1^f* allele into the *Tsc1^A* allele and conversion of the quiescent *R26R* allele into the activated form. Activated *R26R* produces β -gal protein, which indelibly labels recombined cells (green). (c, left) A non-*Gbx2^{CreER}*-expressing cell, such as one in the cerebral cortex, possesses the *Tsc1^f* and *R26R* allele and produces functional TSC1/2 protein, but do not express CreER protein. (c, right) Upon tamoxifen exposure, tamoxifen enters the cell, but has no CreER to bind. Thus, the *Tsc1^f* allele remains functional and TSC1/2 protein continues to be produced by the cell. Additionally, the *R26R* allele remains quiescent, so the cell produces no β -gal.

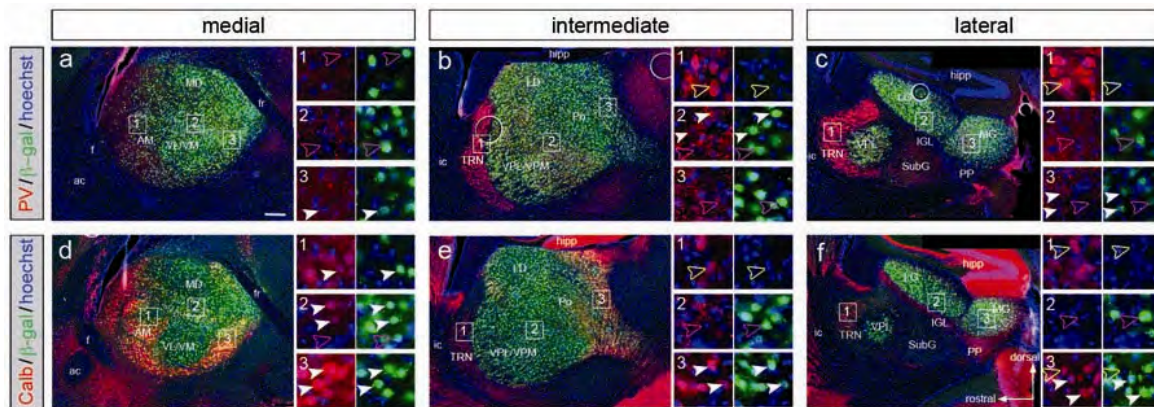


Supplemental Figure 2. Spatial control over *Tsc1*^{fl} allele recombination. (a,b) Control (a, *Tsc1*^{+/+}) and mutant (b, *Tsc1*^{Δthal/Δthal}) embryos were exposed to tamoxifen at E12.5 to induce CreER-mediated recombination of the *Tsc1*^{fl} allele and were harvested at E17.5. (a', b') 12um sagittal brain sections were manually microdissected to collect thalamic tissue (red circle) as well as control tissue from the cerebral cortex (yellow circle). (c) Tissue was lysed, and PCR was performed to detect the three alleles of *Tsc1*: *Tsc1*⁺ (295bp), *Tsc1*^{fl} (486bp), and *Tsc1*^{Δthal} (368bp). Conversion of the *Tsc1*^{fl} allele into the *Tsc1*^Δ allele is seen only in the thalamic tissue where *Gbx2*^{CreER} is expressed, but not in the cortical tissue, where there is no CreER expression. Conversely, *Tsc1*⁺ is unaffected in both the cortical and thalamic tissue samples, as expected.

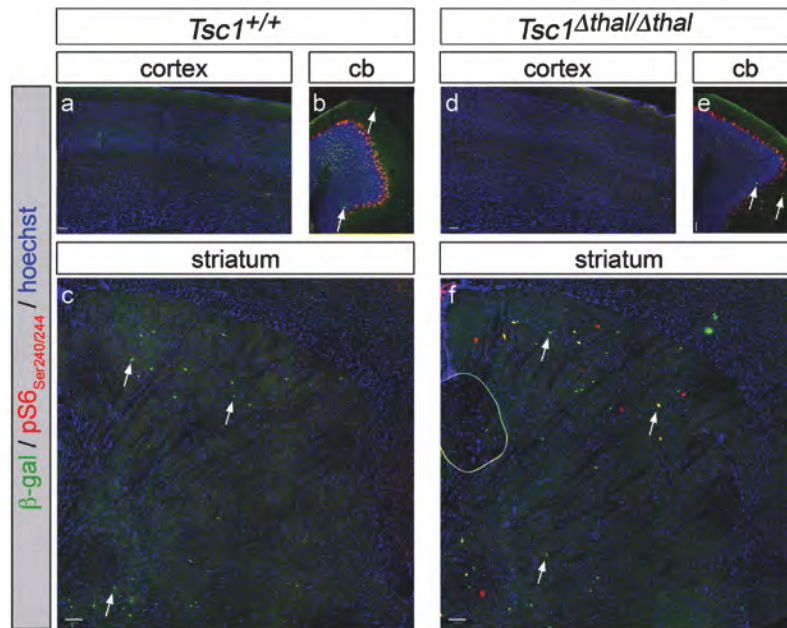


Supplemental Figure 3. *Gbx2*^{CreER} at mediates recombination extensively throughout the thalamus. Tamoxifen was administered to pregnant females harboring *Gbx2*^{CreER};R26R embryos at E12.5 (a,b) or E18.5 (c,d). Upon reaching adulthood, sagittal brain sections were stained for β -gal (green) to detect recombined cells from the *Gbx2*^{CreER} lineage. Although recombination is much more extensive at E12.5 than at E18.5 (particularly

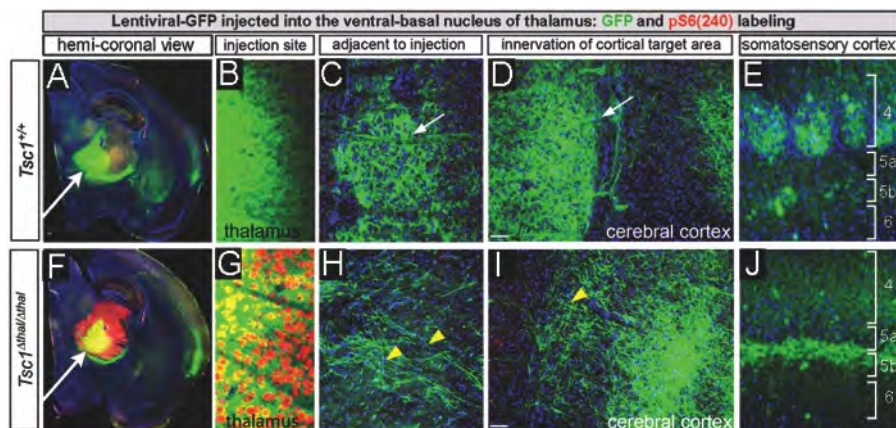
laterally), the overall thalamic regions of recombination are similar. Hoechst nuclear counterstain is blue. Scale bar: 240 μ m.



Supplemental Figure 4. *Gbx2^{CreER}* lineage gives rise to an unbiased population of thalamic relay neurons. Tamoxifen was administered to pregnant females harboring E12.5 *Gbx2^{CreER};R26R* embryos. Once pups reached adulthood, they were intracardially perfused. Sagittal brain sections from the medial, intermediate, and lateral thalamus were immunostained for β -gal (**a-f**, green) and PV (**a-c**, red) or Calb (**d-f**, red). Cells that underwent recombination of the *R26R* allele express β -gal were present throughout the medial and intermediate thalamus. Laterally, recombination occurred in the VP, MG, and LG nuclei, but not the SubG, IGL, or PP. Notably, the PV+ thalamic reticular nucleus (TRN) was completely devoid of β -gal (b, c). **(1-3)** High magnification examples of recombined cells that also expressed the respective marker proteins (white arrowheads), recombined cells that did not express the marker proteins (purple arrowheads), and non-recombined cells that expressed the respective marker proteins (yellow arrowheads). n=3 animals. Scale bar: 270 μ m. AM, anteromedial nucleus; MD, mediodorsal nucleus; VL, ventrolateral nucleus; VM, ventromedial nucleus; TRN, thalamic reticular nucleus; VPL, ventroposterolateral; VPM, ventroposteromedial; LD, laterodorsal; Po, posterior thalamic nuclear group; LG, lateral geniculate; MG, medial geniculate; SubG, subgeniculate; hipp, hippocampus; f, fornix; ac, anterior commissure; fr, fasciculus retroflexus; ic, internal capsule.

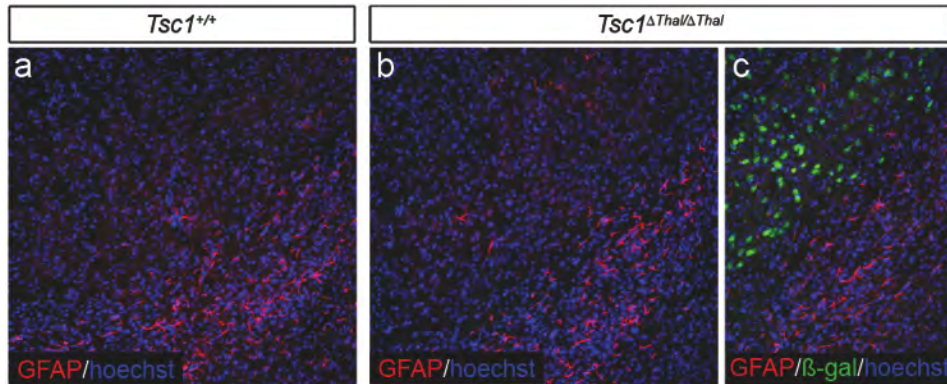


Supplemental Figure 5. Sparse extra-thalamic recombination in the *Gbx2^{CreER}* brain. (a-f) β -gal IHC (green) indicates lack of cellular recombination in the cortex (a, d) and very sparse recombination within the cerebellum (b,e) and striatum (c,f). (d-e) p-S6_{Ser240/244} IHC (red) shows that some of the β -gal cells also respond to *Tsc1* inactivation by undergoing mTOR dysregulation. Purkinje cells of the cerebellum express high basal levels of p-S6_{Ser240/244} (b,e). It has been previously reported that there is also *Gbx2^{CreER}* expression within the spinal cord at E12.5⁵⁰.



Supplemental Figure 6. Altered distribution of thalamic projections in the internal capsule and cerebral cortex of *Tsc1^{Δthal/Δthal}* mutants. Lentiviral-GFP was stereotactically injected into the ventrobasal nuclei of the thalamus. After two weeks the brains were harvested, sectioned, and immunostained for GFP (green) and p-S6_{Ser240/244} (red). GFP+ thalamic axons can be seen exiting the control (a,b) or mutant thalamus (f,g), traversing the striatum (c,h), and entering the cerebral cortex (d,i). Characteristic whisker barrels of the somatosensory cortex can be clearly delineated by the preferential thalamocortical innervation in control

brains (e), whereas this barrel pattern is much less apparent in the *Tsc1^{Δthal/Δthal}* mutant brain (j) and the GFP+ projections instead stratify in deeper cortical layers.



Supplemental Figure 7. Astrocytes are unaffected in E12.5 *Tsc1^{Δthal/Δthal}* mutants. *Tsc1^{+/+}* and *Tsc1^{Δthal/Δthal}* adult brain sections were stained for GFAP, and astrocyte marker, to determine if gliosis occurred as a result of early *Tsc1* inactivation. No changes in GFAP were observed.

Supplemental Video 1. *Tsc1^{Δthal/Δthal}* mouse is shown during a typical seizure. Note that seizure begins with clamping of the hindpaw, then loss of upright posture resulting in a twisting convulsive motion. Afterwards, upright posture is regained and, after a brief pause, normal activity is resumed.

Supplemental Video 2. White *Tsc1^{Δthal/Δthal}* mouse (middle of cage) is shown as an example of characteristic long bouts of inactivity. These periods of inactivity lasts up to 2 minutes at a time, with brief movements only elicited upon physical interaction by cagemates or by experimenters.

Elizabeth Normand¹, Catherine Browning², and Mark Zervas²

¹Department of Neuroscience and ²Department of Molecular Biology, Cell Biology and Biochemistry, Division of Biology and Medicine, Brown University, 70 Ship St., Providence, RI 02903

*Author for correspondence

Address:

Laboratory of Developmental Neurobiology, Genetics and Neurological Disease
Department of Molecular Biology, Cell Biology and Biochemistry
Division of Biology and Medicine

Box G-E436
Brown University
Providence, RI 02912

Courier delivery:
Laboratories for Molecular Medicine
70 Ship Street, Rm. 436
Providence, RI 02903

email: Mark_Zervas@brown.edu
Tel: 401-863-6840
Fax: 401-863-9653
Web page: http://research.brown.edu/myresearch/Mark_Zervas

Running title: Genetic marking of neural circuits

Abstract

Gene expression is a dynamic process where the onset and duration of gene expression is highly coordinated during development to ensure the proper allocation of cell types and tissues. Equally important is how cohorts of neurons establish axonal projections that innervate terminal target sites. We sought to bridge the temporal dynamics of gene expression within a specific genetic lineage and the establishment of the neuronal circuits derived from early expressing cohorts of progenitors. A central goal was to be able to accomplish genetic inducible circuit mapping non-invasively and with commonly available CreER/loxP technology. We specifically genetically marked thalamic neuron progenitors that expressed the transcription factor *Gbx2* at an early embryonic stage and tracked the formation of lineage-derived thalamocortical axons during embryogenesis and at an early postnatal stage. We show that specificity of lineage marking provides a high degree of clarity in following neural circuit development. We also show how the onset and duration of gene expression can be used to delineate subsets of neural circuits. Finally, we uncovered a novel contribution of *Gbx2*-expressing progenitors to midbrain dopamine neurons and dopaminergic axons of the medial forebrain bundle. We anticipate that this system can be instructive in elucidating changes in neural circuit development in the context of normal development and in mutant mice in which circuit formation is altered.

Introduction

The relationship between a specific gene expressed in progenitors during development and the terminal cell fate of these progenitors is referred to a genetic lineage . An important aspect of genetic lineage is how the timing of gene expression within the lineage helps shape the distribution and ultimate cell fate in mature tissues including the nervous system (Dymecki and Kim, 2007; Joyner and Zervas, 2006). An important aspect of nervous system development is that axons of neurons anatomically bind functional domains through the establishment of neural circuits. An important developmental problem is forging a link between progenitors that express genes with temporal precision and establishing neural circuits related to the lineage derived neurons. There have been recent advances in tackling the problem of neural circuit formation using mice as a model system (reviewed in Luo et al., 2008 and see Lo and Anderson, 2011), but there are relatively few examples of marking neural circuits and establishing easily discernible point to point labeling of axonal connections based on temporal gene expression in mice. Thus, a desirable feature of circuitry mapping would be the use of a genetic based system that can be used to mark progenitors with spatial and temporal control, conferring a high fidelity of marking, and that could be readily used to assess genetic mutant mice. We previously showed that an inducible *CreER* recombinase based system and conditional GFP reporter allele allowed for the detection of lineage-derived axons (Ellisor et al.,

2009; Hagan and Zervas 2011]). Here, we used a well-characterized *CreER* line in combination with a commercially available conditional reporter to characterize distinct stages of axonal development and we specifically mark and track developing thalamic neurons and their emerging circuits during *in vivo* development. We also show that a genetics approach can elucidate temporal dynamics of gene expression and specific neural circuits *in vivo*. We anticipate that the ease and robustness of this approach will advance our understanding of neural circuit formation in normal development and in genetic mutant mice.

Experimental Methods

Mice and Fate Mapping. *Gbx2^{CreER}* mice were bred to *R26^{tdTomato}* reporter mice to generate *Gbx2^{CreER-ires-eGFP};R26^{tdTomato}* mice that were subsequently bred to Swiss Webster mice (Taconic) for genetic inducible fate mapping (GIFM) experiments. *Gbx2^{CreER-ires-eGFP}* mice (Chen et al., 2009) were generously provided by James Li (UCHC) and the *Rosa26^{tdTomato}* (*Rosa26^{lox-STOP-lox-tdTomato}*) (Madisen et al., 2010) mice were purchased from Jackson Laboratories. Adult mice that were between four and six weeks of age were set up at the end of the day (1600-1700 hours) and checked for the presence of a vaginal plug each morning at 0900 hours. The presence of a plug was considered 0.5 days post conceptus or embryonic day (E)0.5. Pregnant female mice harboring embryos at E9.5 mice were administered 4mg (200 μ l) of tamoxifen from a stock solution of tamoxifen in corn oil (20mg/ml) at 0900 hours by oral gavage as previously described (Ellisor et al., 2009; Brown et al., 2009; Ellisor and Zervas, 2010). Litters were then dissected at E12.5 or E18.5. An additional cohort of mice that were allowed to go to term were sacrificed at postnatal day (P)7. All mice were housed, handled, and euthanized in accordance with IACUC guidelines at Brown University.

Tissue Processing. Embryos were dissected in PBS over ice and a small tail biopsy was used for genotyping. P7 mice were perfused with saline and 4% paraformaldehyde (PFA) and the brains removed as previously described (Brown et al., 2009; Hagan and Zervas, 2011). Embryos and brains were fixed in PFA overnight at 4 °C. Subsequently, the tissue was rinsed in PBS and immersed in 15% sucrose and 30% sucrose until submerged. Tissues were embedded in Optimal Cutting Temperature (OCT) in cryomolds. Subsequently the OCT/cryomolds were immersed in a polypropylene beaker containing 2-methyl-butane that was immersed in a vessel containing liquid nitrogen until the temperature reached -150°C as described (<http://www.adam.com.au/royellis/fr.htm>). Sections were obtained on a Leica cryostat and mounted on slides.

Immunocytochemistry and microscopy (ICC). Sections (12µm) were rinsed in PBS for 5 min and fixed in 4% PFA in PBS for 5 min. Slides were then rinsed 3 times in 0.2% TritonX-100 in PBS (PBT) for 5 min each and blocked in 10% donkey serum in PBT for 2 h at room temperature in a humid box. Sections were labeled with an anti-DsRed antibody that detects the protein product generated by the recombinant *R26^{tdTomato}* reporter allele (anti-dsRed Ab from Clontech, Cat # 632496, 1:500 in 10% donkey serum in PBT). We also used an anti-TH primary antibody (Chemicon; Billerica, MA; Cat# AB152, 1:500 in 10% donkey serum in PBT) to detect dopamine neurons and their axons at E12.5. Appropriate, species matched Alexa secondary antibodies (Molecular Probes) were prepared at a concentration of 1:500 in 1% donkey serum in PBT. Sections were incubated in 300µl of secondary antibody solution for two hours at room temperature, washed with PBT five times for ten minutes each, and counterstained with .01% Hoechst 33342 (Molecular Probes; Cat # H-3570) in PBS for five minutes in the dark. Slides were washed two times with PBS for 2 min each, dried and coverslipped. Data were collected with a Leica DM600B epifluorescent microscope using Volocity 5.1 imaging software (Improvision). Low magnification images were captured with a Leica MZ16F stereo fluorescent dissecting microscope using PictureFrame software and high magnification images were obtained using a motorized stage with a 20x objective. True magnifications are indicated by scale bars. All images were pseudo colored live as part of the acquisition palettes. Imaging data sets were exported to Adobe Photoshop and montages of representative data were generated.

Results

We administered tamoxifen to E9.5 *Gbx2^{CreER-ires-eGFP}* embryos to mark thalamic progenitors *in vivo* (Chen et al., 2009). We coupled this line with *R26^{tdTomato}* conditional reporter mice because they provide a robust readout of Cre-mediated recombination (Madisen et al., 2010). In the absence of tamoxifen, CreER protein is sequestered in the cytoplasm and recombination of conditional alleles does not occur (Ellisor et al., 2009; Ellisor and Zervas, 2010). However, by delivering tamoxifen to pregnant female mice we can control the release of CreER from sequestration, which frees it to translocate to the nucleus where it mediates recombination in same site oriented *loxP* sites that flanked a *stop* cassette in the reporter allele timing (reviewed in Joyner and Zervas, 2006). Thus, tamoxifen administrations allowed us to control the timing of the recombination event and cell marking within the *Gbx2* lineage.

We first analyzed embryos at E12.5, which showed thalamic neurons derived from the *Gbx2* lineage (Fig. 1A,B). The marked neurons had axons that emerged from the thalamus and formed a thick proximal fascicle (Fig. 1A-C). The *Gbx2*-derived axonal projections terminated at a distal limit in the proximity of the thalamocortical intermediate target zone (Fig. 1D) consistent

with thalamocortical axon guidance (Inan and Crair, 2007). A second cohort of *Gbx2*-derived neurons were in the ganglionic eminence (Fig. 1E). In addition to the thalamocortical projections, there was a more ventrally located loose axonal fiber in what appeared to be the medial forebrain bundle (Fig. 1A, MFB). The *Gbx2*^{CreER-ires-eGFP;R26^{tdTomato}} allelic configuration allows for the determination of progenitors that expressed *Gbx2* at the stage of marking and whether they continued to express *Gbx2* at the stage of analysis. We previously found that this approach was instructive in determining how the timing and duration of *Gbx2* expression shaped early spinal cord development (Luu et al., 2011). We therefore assessed dynamic gene expression and early thalamic circuits using this analysis and identified neural circuits that were derived from early *Gbx2* expressing progenitors marked at E9.5 (tdTomato+, red) and neurons that were expressing *Gbx2*(GFP) at the time of analysis (GFP+ neurons and their axons, green). Interestingly, the thalamocortical axons at E12.5 were derived from neurons that had early and persistent *Gbx2* expression (tdTomato+/GFP+, yellow) (Fig. 2A,A'). In contrast, the *Gbx2*-derived axons in the putative medial forebrain bundle did not continue to express *Gbx2*(GFP) (Fig. 2A). We then used antibody labeling to detect tyrosine hydroxylase (TH) which labels midbrain dopamine neurons and TH+ axons that course along the medial forebrain bundle (Blakely et al., 2011; Vitalis et al., 2000). Surprisingly, the *Gbx2*-derived axons (dsRed+) in the medial forebrain bundle were also TH+, which suggested that dopamine neurons were derived *Gbx2*-derived progenitors marked at E9.5 (Fig. 2B,B',3). We validated that midbrain dopamine neurons were also dsRed+ (Fig. 2B*).

The *Gbx2* lineage-derived neurons marked at E9.5 continued to populate the thalamus at E18.5 (Fig. 3A,B). These thalamic neurons had axons that exited the ventral aspect of thalamus (Fig. 3C) and traversed ventrally and rostrally as fascicles that passed through the ventral half of the striatum (Fig. 3D). The bundles de-fasciculated as they entered the cerebral cortex and formed axonal branches but did not yet innervate the cortical layers (Fig. 3E). In addition, the tdTomato (dsRed+) projections could be used to track entire axonal bundles en route to the deep cortical layers in more lateral sections. Finally, by P7 thalamic neurons derived from *Gbx2*-expressing progenitors marked at E9.5 were distributed broadly in the thalamus and had characteristic thalamic morphologies and broad sweeping fascicles that emerged from the lateral extent of the thalamus and entered the internal capsule (Fig. 4A-C). The fascicles remained well organized and appeared as parallel-oriented fibers with numerous small terminal ramifications throughout and at the anterior-dorsal extent of the caudate/putamen (Fig. 4D). Significant cohorts of thalamocortical projections passed through the internal capsule and caudate/putamen as smaller bundles compared to their entrance into the internal capsule, but retained a parallel orientation with each other as they entered into layer 6b of the cerebral cortex (Fig. 4E,F). In parallel sections (Fig. 4H,I) the *Gbx2*-derived axons formed a dense fiber tract

with long longitudinal processes positioned along the rostral-caudal axis (Fig. 4I). Once the thalamocortical axons innervated the cerebral cortex, the fibers apparently de-fasciculated and formed numerous fine ramifications in the cortex (Fig.s 3F and 4). In somatosensory cortex, the *Gbx2*-derived projections formed dense axonal clusters that established the rudimentary somatosensory barrels (Fig. 4C).

Discussion

The thalamus is composed of both locally projecting interneurons and long-distance projection neurons (Jones 2007). Physical tracing methods have been instructive in elucidating the formation of thalamocortical axons and is a well described process that begins with thalamic axons emanating from the thalamus and halting at intermediate target sites. Subsequently, thalamic axons turn toward and innervate the cerebral cortex (Bayer and Altman, 1991; Adams and Baker, 1995; Inan and Crair, 2007; Vanderhaeghen and Polleux, 2004). It has been shown that the *Gbx2* lineage contributes to thalamic neurons and that *Gbx2* is required for the proper formation of thalamic axonal projections (Hevner et al., 2002; Miyashita-Lin et al., 1999). In addition, *Gbx2* is required cell non-autonomously for thalamic development (Chen et al., 2010). However, establishing a relationship between the timing of gene expression, genetic lineage and neural circuit formation in general using genetic based methods and specifically within the *Gbx2* lineage has not been demonstrated. Thus, we sought to use genetic inducible fate mapping as an approach to demonstrate whether the early expression of *Gbx2* in thalamic neuron progenitors was related to the formation of long distance axonal circuits that eventually innervate cortical targets. We marked *Gbx2* expressing progenitors at E9.5 and analyzed early patterns of axonal growth after three days. We observed clearly labeled *Gbx2* lineage derived thalamocortical axons that exited the thalamus in thick fascicles and were abrogated at the ganglionic eminence consistent with previous physical axonal tracing methods (Jones 2007). By E18.5 the *Gbx2* derived axons entered the striatum as thick fascicles and formed a rich axonal plexus. Upon exiting the caudate/putamen, well-defined axonal tracts entered the deep cortical layers with fine axons that begin to ramify into more superficial layers. At P7, the axons that entered the cortex formed an axonal tract that traversed the rostral-caudal axis. While at E18.5 only fine axons innervated more superficial cortical layers, by P7 the projections establish a broad zone of termination in layer 4 of cortex. In the somatosensory cortex, the projections coalesce as the rudimentary layer 4 barrel structures.

During the course of our analysis, we also observed a second surprising *Gbx2* lineage derived axonal tract located ventrally in the medial forebrain bundle. Thus, we show for the first time that a portion of the medial forebrain bundle axons are derived from *Gbx2* expressing

progenitors that contribute to dopamine neurons. It is well known that *Gbx2* expression defines a domain that is posterior to the germinal zone of ventral midbrain progenitors (Wassarman et al., 1997; Martinez-Barbera et al., 2001; Li and Joyner, 2001; Li et al., 2002) although a recent study showed that *Gbx2* is also transiently expressed in the ventral midbrain primordia (Sunmonu et al., 2011), which is the source of midbrain dopamine neurons (Brown et al., 2011, Hayes et al., 2011). We show here that thalamocortical axons were derived from neurons that had early and persistent expression of *Gbx2* (tdTomato+/GFP+, yellow). In contrast, the dopaminergic axons in the medial forebrain bundle were derived from progenitors that expressed *Gbx2* only early and transiently (at E9.5, but not at E12.5). Thus, this genetic circuit mapping approach makes it possible to link differential timing of gene expression and specific neural circuits within a specific genetic lineage. Finally, we show that a genetic based approach is highly effective at marking and following neural circuit formation *in vivo*. This approach has distinct advantages including that it is not invasive, is highly reproducible forges a link between temporal gene expression during embryogenesis and postnatal neural circuits.

Acknowledgements

This work was supported by a Department of Defense CDMRP grant (TS110067, MZ) and the Brown University Department of Neuroscience training grant (NS062443-02).

Figure Legends

Fig. 1. Genetic marking uncovers early neural circuit formation.

Tamoxifen was administered to *Gbx2^{CreER-ires-eGFP};R26^{tdTomato}* embryos at E9.5 and analyzed at E12.5. **A.** Sagittal section immunolabeled with an anti-dsRed antibody to detect neurons in the thalamus (thal) and ganglionic eminence (ge) that underwent recombinations. Neuronal projections were also labeled with the reporter allele and allowed for the detection of a thick fascicle concomitant with thalamocortical axon bundle (TCA) that coursed rostrally and were halted at the ganglionic eminence. A loose axonal bundle was also detected in the vicinity of the medial forebrain bundle (MFB). The inset shows the region of analysis; prosencephalon (pros), mesencephalon (mes), rhombomere 1 (r1). **B.** *Gbx2*-derived neurons in the thalamus (dsRed+, arrowheads) and a thick axonal plexus (arrows). **C.** TCA of *Gbx2*-derived neurons marked at E9.5 exited the thalamus as a thick bundle. **D.** TCA termination at distal to the thalamus. **E.** *Gbx2*-derived neurons in the ge. In B-E, sections were counterstained with hoechst (blue).

Fig. 2. Timing of gene expression define subsets of neural circuits within a defined genetic lineage.

Tamoxifen was administered to *Gbx2^{CreER-ires-eGFP};R26^{tdTomato}* embryos at E9.5 and analyzed at E12.5. **A.** Sagittal section immunolabeled with anti-dsRed and anti-GFP antibodies to detect thalamic neurons that, respectively, expressed *Gbx2* at E9.5 (dsRed+, red) and currently expressed *Gbx2* at E12.5 (GFP+, green). Sections were counterstained with hoechst (blue). Neurons in the thalamus (thal) and TCA (yellow arrows) were dsRed+/GFP+ (yellow) indicating that they were derived from neuronal progenitors that expressed *Gbx2* at E9.5 and continued to express *Gbx2* at E12.5. The axons in the medial forebrain bundle were dsRed+.GFP- (red arrows) indicating that these projections were related to neurons that expressed *Gbx2* early, but ceased expressing *Gbx2* by E12.5. **A'**. Thalamus from same sample but at more medial location. **1,2.** High magnification panels of regions of interest shown in A. **B.** Sagittal section immunolabeled with anti-dsRed and anti-tyrosine hydroxylase (TH) antibodies to detect neurons that expressed *Gbx2* at E9.5 (dsRed+, red) and to identify dopamine neurons (TH+, green), respectively. Neurons in the thal and TCA were dsRed+ consistent with adjacent section in A. The MFB contained TH+ dopaminergic axons (white arrows). **B'**. High magnification view of thal and dopaminergic axons coursing ventral the the thal. The TH+ projections were also dsRed+ but were much fainter than the neurons in the thalamus. **3.** High magnification panel of region 3 with the red signal increased to observe the projections. *. The asterisk indicates a region that is caudal and medial to B,B' showing that midbrain dopamine neurons derived from the *Gbx2* lineage marked at E9.5 (dsRed+/TH+, yellow) that projected along the MFB.

Fig. 3. Maturation of lineage derived neural circuits. Genetic marking uncovers early neural circuit formation.

Tamoxifen was administered to *Gbx2^{CreER-ires-eGFP};R26^{tdTomato}* embryos at E9.5 and analyzed at E18.5. **A.** Sagittal section immunolabeled with an anti-dsRed antibody to detect neurons in the thalamus (thal) that underwent recombination. Sections were counterstained with hoechst (blue). The thalamocortical axon bundle (TCA) traversed the striatum (str) and entered the deep layers of the cerebral cortex (ctx). **B.** Thalamic neurons that expressed *Gbx2* at stage of marking were becoming morphologically distinct. **C.** The TCA exited the thal as thick well-defined fascicles that turned rostrally (arrow). **D.** The *Gbx2* derived projections entered the striatum (arrows) and formed a fine network of axonal terminals which was in contrast to the TCA marked at the same stage but analyzed at E12.5 (See Fig. 1). **E.** TCA that exited the striatum were fine and ramified the the deep cortical layer. **F.** In an a section adjacent to panels A-E the *Gbx2*-derived TCA could be followed through the striatum and innervating the deep cortical layers with fine axonal branches that were progressively sparser in layers superficial to cortical layer 6.

Fig. 4. Target innervation of genetic lineage derived neural circuits.

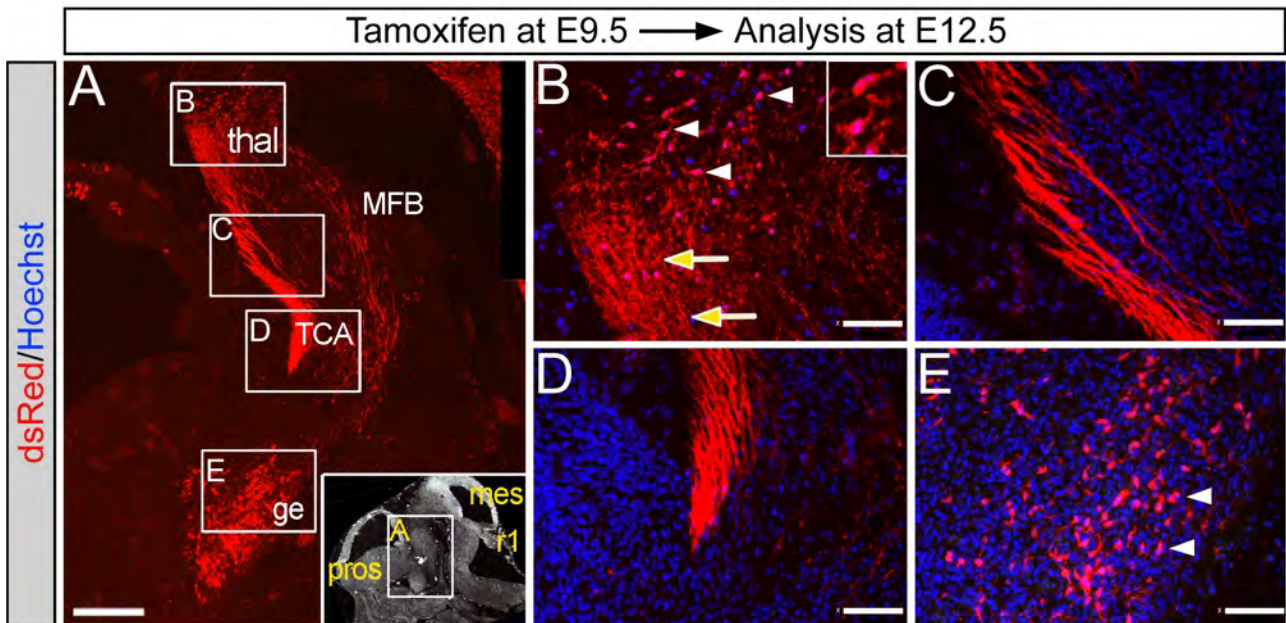
Tamoxifen was administered to *Gbx2^{CreER-ires-eGFP};R26^{tdTomato}* embryos at E9.5 and analyzed at P7. **A.** Sagittal section immunolabeled with an anti-dsRed antibody detected neurons and the thalamocortical axon bundle (TCA) derived from the *Gbx2* lineage marked at E9.5. Sections were counterstained with hoechst (blue). *Gbx2*-derived TCA traversed the striatum (str) as thick bundles where they branched and formed fine axonal terminations. The TCA exited striatum and innervated the cerebral cortex (ctx). **B.** Neuronal progenitors that expressed *Gbx2* at E9.5 contributed to mature thalamic neurons that were distributed in the thal. **C.** Numerous thick TCA exited the thal. **D.** TCA traversed the entire distance of the str as thick bundles with fine axonal branches that established *Gbx2*-derived plexus in the caudate/putamen of the str. **E,F.** Upon exiting the str, the TCA projections were thinner in comparison to when they entered and traversed the str. The TCA then formed a a dense plexus in deep cortical layers. **G.** *Gbx2*-derived neurons remaining in close proximity, but ventral to the thal. **H,I.** In an adjacent sagittal section to A-G, *Gbx2*--derived axons traversed the rostral-caudal axis as long axonal bundles that were oriented parallel to the ventral surface. In somatosensory cortex, the axons coalesced in a fingerprint pattern, consistent with the early formation of barrel cortex.

References

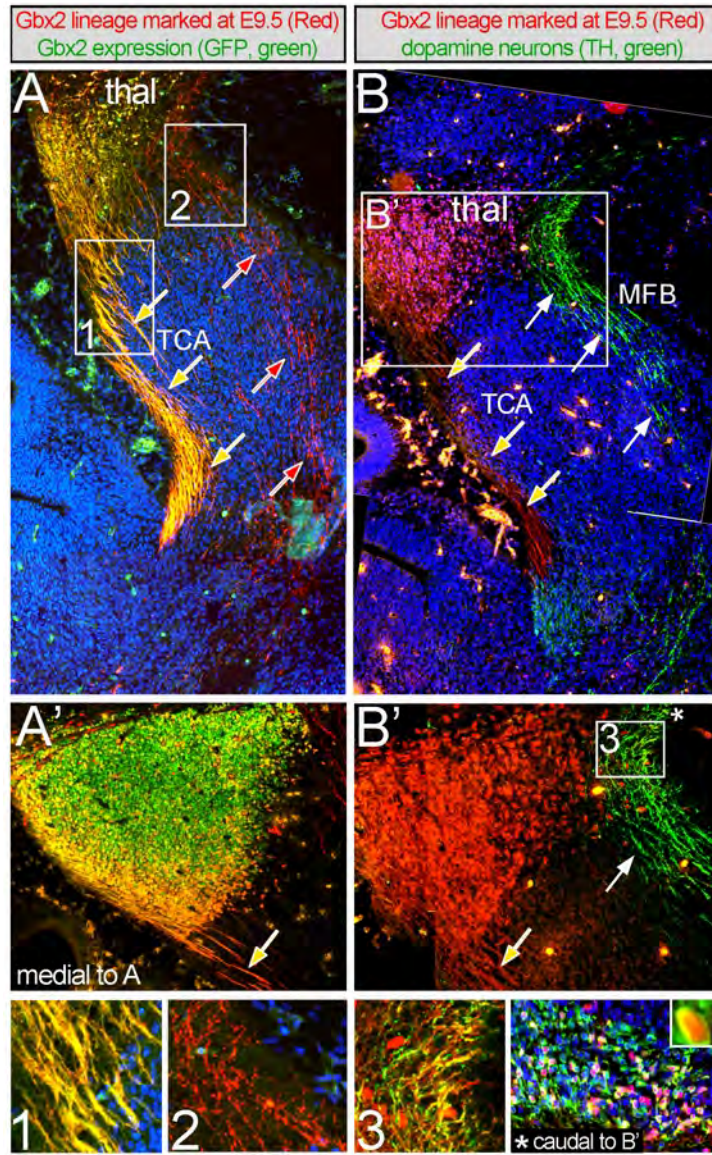
- Adams, N.C., and Baker, G.E. 1995. Cells of the perireticular nucleus project to the developing neocortex of the rat. *J Comp Neurol* 359, 613-626.
- Bayer, and Altman 1991. *Neocortical Development* (New York, NY: Raven Press).
- Brown, A., Brown, S., Ellisor, D., Hagan, N., Normand, E., and Zervas, M. (2009). A practical approach to genetic inducible fate mapping: a visual guide to mark and track cells in vivo. *J Vis Exp* , pii: 1687.
- Brown, A., Machan, J.T., Hayes, L., and Zervas, M. 2011. Molecular organization and timing of Wnt1 expression define cohorts of midbrain dopamine neuron progenitors in vivo. *J Comp Neurol* 519, 2978-3000.
- Chen, L., Chatterjee, M., and Li, J.Y. 2010. The mouse homeobox gene Gbx2 is required for the development of cholinergic interneurons in the striatum. *J Neurosci* 30, 14824-14834.
- Chen, L., Guo, Q., and Li, J.Y. 2009. Transcription factor Gbx2 acts cell-nonautonomously to regulate the formation of lineage-restriction boundaries of the thalamus. *Development* 136, 1317-1326.
- Dymecki, S.M., and Kim, J.C. 2007. Molecular neuroanatomy's "Three Gs": a primer. *Neuron* 54, 17-34.
- Ellisor, D., and Zervas, M. 2010. Tamoxifen dose response and conditional cell marking: Is there control? *Mol Cell Neurosci* 45, 132-138.
- Ellisor, D., Koveal, D., Hagan, N., Brown, A., and Zervas, M. 2009. Comparative analysis of conditional reporter alleles in the developing embryo and embryonic nervous system. *Gene Expr Patterns* 9, 475-489.
- Hagan, N., and Zervas, M. 2011. Wnt1 expression temporally allocates upper rhombic lip progenitors and defines their terminal cell fate in the cerebellum. *Mol Cell Neurosci* 49, 217-229.
- Hevner, R.F., Miyashita-Lin, E., and Rubenstein, J.L. 2002. Cortical and thalamic axon pathfinding defects in Tbr1, Gbx2, and Pax6 mutant mice: evidence that cortical and thalamic axons interact and guide each other. *J Comp Neurol* 447, 8-17.
- Inan, M., and Crair, M.C. 2007. Development of cortical maps: perspectives from the barrel cortex. *Neuroscientist* 13, 49-61.
- Jones, E. 2007. *The thalamus*, Jones, eds. (Cambridge ; New York: Cambridge University Press).
- Joyner, A.L., and Zervas, M. 2006. Genetic inducible fate mapping in mouse: Establishing genetic lineages and defining genetic neuroanatomy in the nervous system. *Dev Dyn* 235, 2376-2385.
- Li, J.Y., and Joyner, A.L. 2001. Otx2 and Gbx2 are required for refinement and not induction of mid- hindbrain gene expression. *Development* 128, 4979-4991.

- Li, J.Y., Lao, Z., and Joyner, A.L. 2002. Changing requirements for Gbx2 in development of the cerebellum and maintenance of the mid/hindbrain organizer. *Neuron* 36, 31-43.
- Lo, L., and Anderson, D.J. 2011. A cre-dependent, anterograde transsynaptic viral tracer for mapping output pathways of genetically marked neurons. *Neuron* 72, 938-950.
- Luo, L., Callaway, E.M., and Svoboda, K. 2008) Genetic dissection of neural circuits. *Neuron* 57, 634-660.
- Luu, B., Ellisor, D., and Zervas, M. 2011. The lineage contribution and role of Gbx2 in spinal cord development. *PLoS One* 6, e20940.
- Madisen, L., Zwingman, T.A., Sunkin, S.M., Oh, S.W., Zariwala, H.A., Gu, H., Ng, L.L., Palmiter, R.D., Hawrylycz, M.J., Jones, A.R., Lein, E.S., and Zeng, H. 2010. A robust and high-throughput Cre reporting and characterization system for the whole mouse brain. *Nat Neurosci* 13, 133-140.
- Martinez-Barbera, J.P., Signore, M., Boyd, P.P., Puellas, E., Acampora, D., Gogoi, R., Schubert, F., Lumsden, A., and Simeone, A. 2001. Regionalisation of anterior neuroectoderm and its competence in responding to forebrain and midbrain inducing activities depend on mutual antagonism between OTX2 and GBX2. *Development* 128, 4789-4800.
- Miyashita-Lin, E.M., Hevner, R., Wassarman, K.M., Martinez, S., and Rubenstein, J.L. 1999. Early neocortical regionalization in the absence of thalamic innervation. *Science* 285, 906-909.
- Sunmonu, N.A., Li, K., Guo, Q., and Li, J.Y. 2011. Gbx2 and Fgf8 are sequentially required for formation of the midbrain-hindbrain compartment boundary. *Development* 138, 725-734.
- Vanderhaeghen, P., and Polleux, F. 2004. Developmental mechanisms patterning thalamocortical projections: intrinsic, extrinsic and in between. *Trends Neurosci* 27, 384-391.
- Vitalis, T., Cases, O., Engelkamp, D., Verney, C., and Price, D.J. 2000. Defect of tyrosine hydroxylase-immunoreactive neurons in the brains of mice lacking the transcription factor Pax6. *J Neurosci* 20, 6501-6516.
- Wassarman, K.M., Lewandoski, M., Campbell, K., Joyner, A.L., Rubenstein, J.L., Martinez, S., and Martin, G.R. 1997. Specification of the anterior hindbrain and establishment of a normal mid/hindbrain organizer is dependent on Gbx2 gene function. *Development* 124, 2923-234.

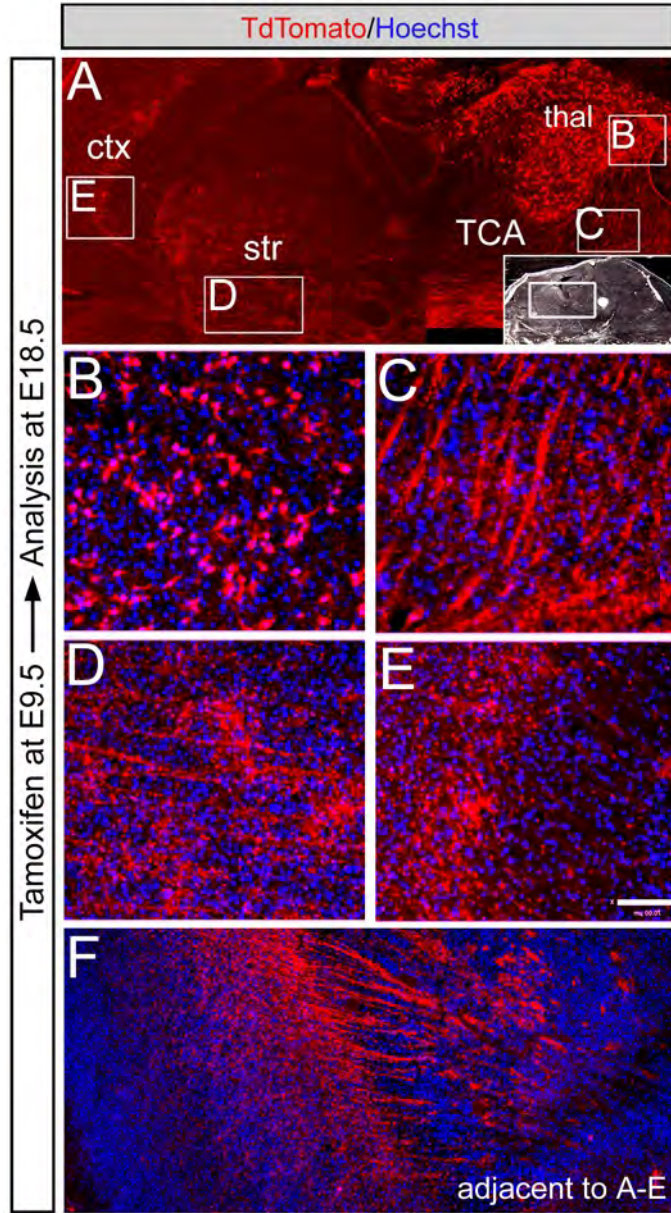
Normand_Figure 1_2012



Normand_Figure 2_2012



Normand_Figure 3_2012



Normand_Figure 4_2012

Tamoxifen at E9.5 → Analysis at P7

